ACS OMEGA

http://pubs.acs.org/journal/acsodf

Article

Effective Adsorption and Removal of Doxorubicin from Aqueous Solutions Using Mesostructured Silica Nanospheres: Box–Behnken Design Optimization and Adsorption Performance Evaluation

Khalid Althumayri, Ahlem Guesmi, Wesam Abd El-Fattah, Lotfi Khezami, Taoufik Soltani, Naoufel Ben Hamadi, and Ahmed Shahat*

Cite This: *ACS Omega* 2023, 8, 14144–14159

Read Online

ACCESS | Metrics & More | Article Recommendations | Supporting Information

ABSTRACT: The aim of this study is to evaluate the efficacy of mesoporous silica nanospheres as an adsorbent to remove doxorubicin (DOX) from aqueous solution. The surface and structural properties of mesoporous silica nanospheres were investigated using BET, SEM, XRD, TEM, ζ potential, and point of zero charge analysis. To optimize DOX removal from aqueous solution, a Box–Behnken surface statistical design (BBD) with four times factors, four levels, and response surface modeling (RSM) was used. A high amount of adsorptivity from DOX (804.84 mg/g) was successfully done under the following conditions: mesoporous silica nanospheres dose = 0.02 g/25 mL; pH = 6; shaking speed = 200 rpm; and adsorption time = 100 min. The study of isotherms demonstrated how well the Langmuir equation and the experimental data matched. According to thermodynamic characteristics, the adsorption of DOX on mesoporous silica nanospheres was endothermic and spontaneous. The increase in solution temperature also aided in the removal of DOX. The kinetic study showed that the model suited the pseudo-second-order. The suggested adsorption method could recycle mesoporous silica nanospheres five times, with a modest reduction in its ability for adsorption. The most important feature of our adsorbent is that it can be recycled five times without losing its efficiency.

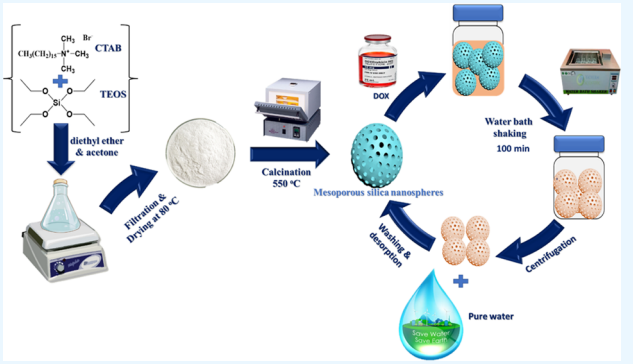

INTRODUCTION

Everything we use every day at home, at work, in our food, etc. contains chemicals. Over the past 200 years, a significant number of chemicals have been introduced into our society without consideration of their toxicological effects on human and animal health as well as the environment. However, we can see that environmental hazards, such as ions, metals, oil derivatives, and pesticides, have been the subject of regulation and monitoring in recent decades, from the 1970s to the present. The most recent focus has also been on emerging contaminants.[1−3] Along with their presence in water resources and wastewater, their transport routes, and accumulation in the environment, scientific knowledge and understanding of the potential health risks emerging pollutants pose to humans and ecosystems is still very limited, which places restrictions on the most effective strategies to prevent or address their presence. Regulations governing the environment, water quality, and wastewater disposal do not cover the majority of developing contaminants.[4,5] The United Nations Educational, Scientific and Cultural Organization (UNESCO) states that there is an urgent need to improve scientific knowledge and adopt appropriate technical and policy approaches to monitor emerging pollutants in the environmental matrixes, assess their potential risks to human health and the environment, and prevent and control their disposal to water resources and the environment.[6]

Cancer is one of the most difficult medical problems today, and it is gaining more and more international attention in both medical practice and research. Technically speaking, cancer is characterized as aberrant cell proliferation brought on by a vicious cell cycle.[7] It has become clear that some environmental and behavioral variables, such as radiation exposure, industrial pollution, smoking, etc., may put people at risk for developing cancer. Looking back on the extensive scientific research done in the field of cancer reveals that while much has been learned about the etiology, epidemiology, symptoms, diagnosis, and treatment of cancer, there is still much work to be done to learn more about this field's many facets, particularly cancer

Received: February 8, 2023
Accepted: March 31, 2023
Published: April 7, 2023

treatment. Today's cancer therapy has become a multidisciplinary area, with contributions from many different scientific disciplines, including cellular and molecular biology, genetics, biophysics, biochemistry, and surgery. Oncologists frequently combine various treatments to treat certain cancers, and common cancer therapy pathways include immunotherapy, chemotherapy, radiation, and surgery.[8−10]

Pharmaceutical medications, known as antineoplastics (therapeutics), are used to treat certain malignancies. Doxorubicin hydrochloride (DOX), a chemotherapy medication, is the most often used treatment for solid tumors. The mode of action brought on by DOX may be divided into two categories: intercalation-induced cell death and DNA rupturing, and free radical generation, or ROS, which damages proteins, DNA, and cell membranes. Due to its poor absorption, severe cardiotoxicity from free radicals, generation of the metabolite doxorubicinol, and mitochondrial disruption, DOX should be avoided. Despite DOX's negative side effects, it is frequently given since antineoplastic therapies are so effective. The initial, untreated DOX waste that is discharged into the environment, together with its metabolites, has a significant impact on aquatic life and has the potential to be detrimental to human health.[11]

Water pollution has grown to be a global issue as human civilization and industrial and agricultural output have progressed.[12−15] Heavy metals, chemical dyes, and antibiotics are just a few of the dangerous elements that are released into the water untreated. Pharmaceutical factories and hospitals manufactured and released a considerable amount of antibiotics. Therefore, the wastewater was found to comprise tetracycline (TC), sulfachloropyradazine (SCP), and doxorubicin hydrochloride (DOX) with high amounts. As a result, hurting aquatic species has a highly negative impact on human health, since such organisms ultimately enter the food chain and end up in the human body.[16,17] Traditional decontamination techniques are still inadequate and ineffective at removing antibiotic contaminants from wastewater treatment facilities because they only effectively remove suspended particles and trace levels of soluble organic pollutants. People are becoming more aware of environmental issues as the idea of environmental protection becomes more widely known. Water environment contamination is one of the most important pollution issues, and hence its solution must be found immediately. Many experts think that adsorption is a method that offers promise in various research on the filtration and treatment of sewage. With the employment of many nanomaterials and their composites for the adsorptive removal of environmental contaminants, significant progress has been made in recent years.[18]

Silica nanospheres have revolutionized modern science with their ability to adsorb large amounts of material. Adsorption is the process of capturing molecules from a gas, liquid, or dissolved solid to the surface of a solid. This type of technology has been employed in the food and beverage industry for decades; however, the introduction of silica nanospheres has opened up an array of new possibilities.[19] Silica nanospheres offer a unique kind of adsorption due to their small pore size and high surface area. These properties allow them to capture molecules on the nanoscale, making them ideal for a wide range of applications. From water purification to drug delivery, these tiny particles are changing the way we think about adsorption and how it can be used to benefit society. The most interesting thing about silica nanospheres is that they can be customized to target-specific molecules, allowing for precise and selective adsorption. This means that scientists can use these particles to filter out unwanted materials, such as bacteria, toxins, and heavy metals, from liquid solutions and make them safe for human consumption. With the ever-increasing number of technological advancements in this field, it is easy to see why silica nanospheres are becoming an essential tool in modern science.[20]

The goal of this study is to look at how DOX behaves in aqueous solutions when it is adsorbed by mesoporous silica nanospheres. To maximize the mesoporous silica nanospheres' ability to adsorptively remove DOX from aqueous solution, a Box−Behnken design and response surface approach were applied. The factors used in the optimization by the Box−Behnken design are DOX concentration, solution pH, amount of adsorber, and time. In order to reduce the nonsignificant contributions of other components, these factors were selected based on preliminary findings.

MATERIAL AND METHODS

The materials, instruments, and methods are described in detail in the Supporting Information.

Optimization Method. Individual and collective consequences of the diverse factors, such as adsorbent dose (A), time (B), solution pH (C), and concentration (D) on the elimination of DOX were looked into using BBD-RSM. The experimental results of DOX removal were statistically analyzed using analysis of variance (ANOVA), as indicated in Table 1.

Table 1. Independent Changeable Range and Level for BBD Runs

variable	symbol	−1	0	+1
dose (g/25 mL)	X1	0.02	0.135	0.25
time (min)	X2	5	52.5	100
pH	X3	2	7	12
initial concentration (mol/L)	X4	0.00028	0.0012	0.0022

RESULTS AND DISCUSSIONS

Characteristics of Mesoporous Silica Nanospheres. Preparing mesoporous silica nanospheres is a delicate and precise process that requires intuition, skill, and patience. To achieve the desired results, a proper combination of solvents must be used judiciously. In this instance, acetone, diethyl ether, and cetyltrimethylammonium bromide (CTAB) are combined in exact proportions to produce a solution that can then be processed into nanospheres.[20,21] The first step is to combine the three solvents. Acetone is added first—its volatile properties give it the ability to penetrate into the structure of the silica while still providing a stable base for other components. Next, diethyl ether serves as an activator, and CTAB acts as a cross-linker, ensuring that the nanospheres remain intact after processing.[22,23] Once the solvents have been properly combined, they are injected into special molds and allowed to sit overnight. Through a process of evaporation and dehydration, a highly porous network of silica spheres forms within the molds. The next morning, the product is carefully removed by calcination from the molds and checked for quality. Despite its complexity, creating mesoporous silica nanospheres is a fascinating and rewarding experience. With each batch, one develops a greater appreciation of how these tiny particles can lead to new insights and technological breakthroughs.[24]

Figure 1A depicts the calcined mesoporous silica nanosphere adsorbent's small-angle X-ray diffraction patterns before and after it had been recycled five times. They exhibit a strong peak at

https://doi.org/10.1021/acsomega.3c00829
ACS Omega 2023, 8, 14144−14159

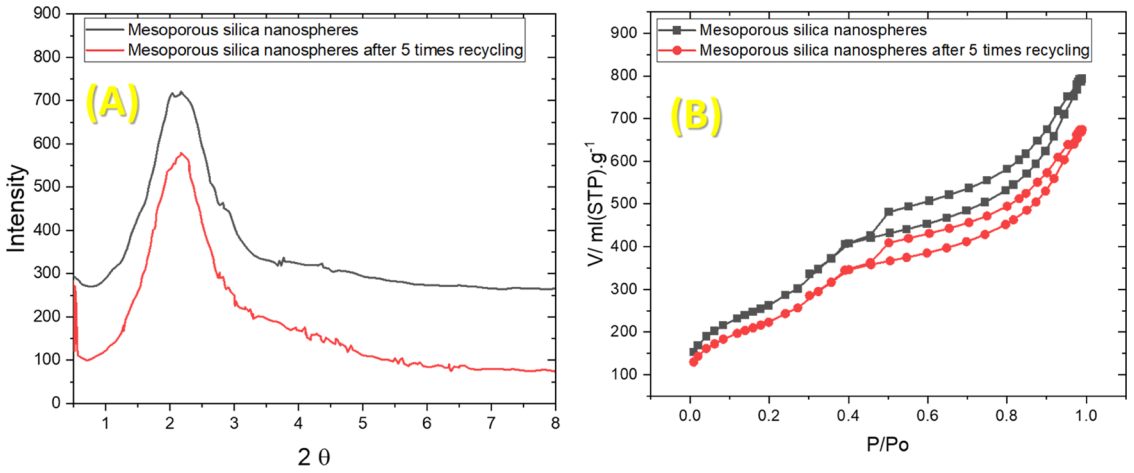

Figure 1. (A) Calcined mesoporous silica nanospheres adsorbent's small-angle X-ray diffraction patterns before and after it had been recycled five times and (B) calcined mesoporous silica nanospheres adsorbent's nitrogen adsorption−desorption isotherms before and after it had been recycled five times.

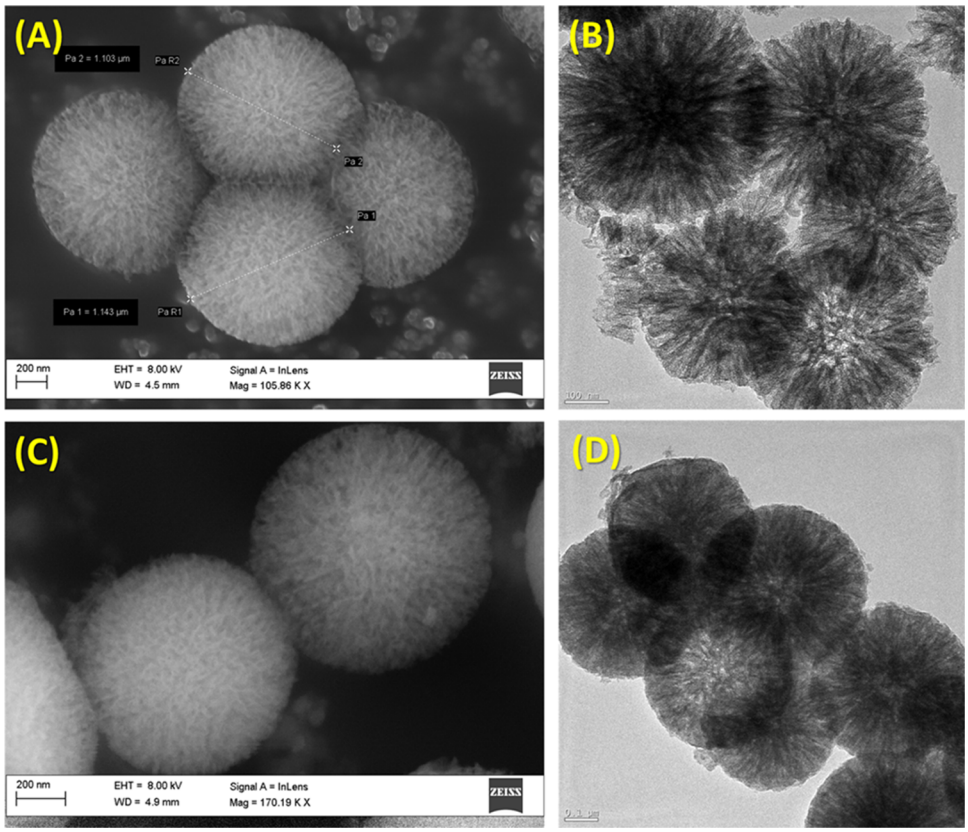

Figure 2. (A) FESEM micrograph of the uniformly sized, spherical-shaped silica nanosphere adsorbent, (B) TEM image represents the highly uniform spherical arrangement of the mesoporous silica nanospheres adsorbent with the mesoporous structure, (C) FESEM micrograph of the mesoporous silica nanospheres adsorbent after five times recycling, and (D) TEM image of the mesoporous silica nanospheres adsorbent after five times recycling.

a 2θ value of 2.3°. As a result, these samples were MCM-41's worm-like counterparts.[24] The lack of the peak in both of them at 2θ = 4.0−5.0° demonstrated a lower degree of order in the mesopores. This was clearly demonstrated by the TEM pictures of the calcined mesoporous silica nanospheres adsorbent before and after five cycles of recycling that are shown in Figure 2B. A typical Bragg's diffraction peak was preserved and showed the durability of the mesoporous silica nanospheres adsorbent network under the employment situation even after the adsorption of DOX molecules onto the mesoporous silica surface and recycling it five times. Additionally, as seen in Figure 1A, both materials' diffraction intensities were largely unaltered.

Mesoporous silica nanospheres adsorbents were shown to be a type IV isotherm by N_2 adsorption−desorption study as shown in Figure 1B. A broad hysteresis loop is also shown occurring at P/P_0 = 0.49−0.99 and a precarious adsorption step occurring at P/P_0 = 0.36. The N_2 isotherms shown in Figure 1B also show that there was a dip into the adsorbent's surface area, which was made up of recycled mesoporous silica nanospheres. The S_{BET} value of the adsorbent after being recycled five times was found

https://doi.org/10.1021/acsomega.3c00829
ACS Omega 2023, 8, 14144−14159

to be 840.86 m^2/g, which was less than the mesoporous silica nanospheres adsorbent (989.25 m^2/g). Similar to the surface area, the recycled adsorbent's pore volume (0.985 L/g) was much smaller than the pore volume of the unusable silica nanospheres adsorbent (1.159 L/g).[25,26] The mesoporous silica nanospheres adsorbent's pore volume and surface area decreased after the mesoporous silica adsorbent had been recycled five times, clearly indicating that the DOX molecules had been stored inside the pores and were evenly spread over the surface. These data also show that the high porosity of the composite adsorbent sample was preserved, which is an important factor in the mesoporous silica's ability to bind DOX.

Figure 2A depicts the FESEM of the mesoporous silica nanospheres adsorbent sample. It is the nanosphere, according to the FESEM measurements. The large slit-like mesopores with a length of 19−28 nm were uniformly dispersed around the nanosphere surface in the TEM images, which depict the shape of nanospheres (Figure 2B). Additionally, the distribution and contrast of the light and dark portions of the nanospheres' edges point to the presence of sizable mesopores with radial orientation.[27]

Point of Zero Charge (PZC). pH, which determined as to which ionic species were present in the DOX solution and the surface charge of the mesoporous silica nanospheres adsorbent, was one of the most crucial parameters for DOX sorption. The pH_{PZC}, at which the positive charges on the surface equal to the negative charges, was used to determine the surface charge of the mesoporous silica nanospheres. It was discovered to have a pH_{PZC} of 6.55 (Figure 3). It was shown that the drug first

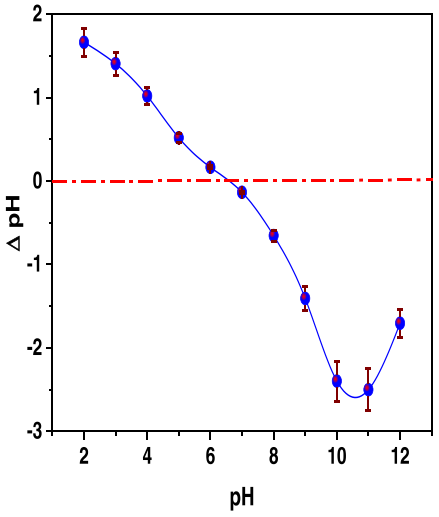

Figure 3. Point of zero discharge of mesoporous silica nanospheres.

adsorbs on the surface of larger holes before diffusing into smaller ones due to the interaction between negatively charged silica centers and positively charged doxorubicin hydrochloride (pH 6). Additionally, it was demonstrated that DOX has a tendency to self-aggregate on silica surfaces. This indicates that the mesoporous silica nanospheres have a positive charge on their surface below this pH due to the protonation of functional groups and a negative charge above this pH. The adsorption of DOX is favored when the surface becomes positively charged at $pH < pH_{PZC}$.

Batch Experiments. *Effect of pH.* Utilizing a stock concentration of 2.5×10^{-3} mol·L^{-1} of DOX, the pH of the aqueous solution was investigated and studied because it affects the adsorbent's surface charge and level of ionization. Figure 4 shows how the starting solution's pH affected the adsorbed DOX molecules. As depicted in Figure 4a, the maximum adsorption for the mesoporous silica nanospheres nanocomposite was seen at pH 6. The adsorption capacity increased as the starting pH was raised from 2 to 6, and the greatest amount of adsorption was recorded at pH 6. The shift in surface charge and the development of limitations to the functional groups may be responsible for the observed reduction in the drug adsorption at pH levels higher than 6. Since the DOX drug's adsorption capability dramatically decreased when its color changed at pH levels over 8.5, it may be assumed that at these pH values, the treatment has actively reacted with the nanocomposite.

Doxorubicin is a chromophoric anthraquinone- and sugar-based anthracycline antitumor antibiotic. The Dox structure contains an amino group; hence, the pH largely determines how the Dox behaves physicochemically. Figure 4b illustrates that the protonated form of the DOX is present in an acidic environment, whereas the nonionized form predominates at neutral and basic pH levels. The best conditions for adsorption research are acidic settings, since DOX is stable in the pH range of 3.0−6.5. It may be assumed that nonionized surface silanol groups cannot interact with completely protonated amino groups of DOX given the chemical makeup of silica surfaces in this pH range. As a result, we cannot anticipate a significant silica surface adsorption capability for DOX molecules in an acidic medium. At neutral pH levels, interactions between nonionized or protonated amine groups and the silica surface may significantly impact the adsorption process.[28−33] The DOX amino acid's positively charged amino groups can engage electrostatically with these ionized silanol groups. Additionally, the creation of hydrogen bonds between nonionized silanol groups and neutral drug molecules may occur, adding to the adsorption process, as seen in Figure 4c.

Effect of Dose. Investigations were done as to how the dose of nanocomposite affected the adsorption of DOX at pH 6. As shown in Figure 5, DOX adsorption substantially increased as the nanocomposite concentration increased from 0.02 to 0.25 g, and at 0.25 g, the DOX adsorption achieved its maximum level. As anticipated, the drug adsorption may be enhanced by increasing the dose of nanocomposite since the active sites are more readily available. In fact, the saturation of the nanocomposite at this concentration and the instability of the aqueous solution at higher dosages than 0.25 g/25 mL are what cause the increase in drug adsorption at this range.

Adsorption Isotherm. Adsorbate behavior and interactions with the adsorbent are revealed by adsorption isotherms, and isotherm investigations shed light on how the adsorbate is distributed between the solution and solid phases during the adsorption equilibrium. Equilibrium revisions that display the capacity of the adsorbent and adsorbate are referred to as adsorption isotherms. The ratio of the amount adsorbed to the amount that remained in solution at equilibrium at a particular temperature is known as the adsorption isotherm. The equilibrium adsorption of chemicals from solutions has been studied using a variety of isotherm models, including Langmuir,[34] Freundlich,[35] Dubinin−Radushkevich,[36] and Temkin.[37]

The homogeneous adsorption energy onto the adsorbent surface is accepted by the Langmuir isotherm model. It is based on the hypothesis that monolayer adsorption could happen on a surface that is even, has a fixed number of similar sites, and has

https://doi.org/10.1021/acsomega.3c00829
ACS Omega 2023, 8, 14144−14159

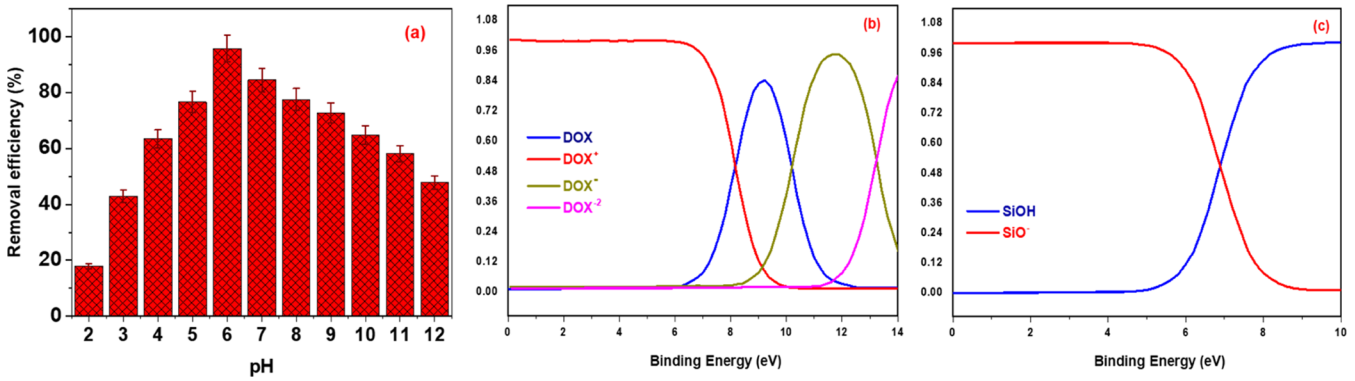

Figure 4. (a) Impact of pH on the adsorption of DOX, (b) distribution graphs of the protolytic forms of DOX, and (c) surface silanol groups.

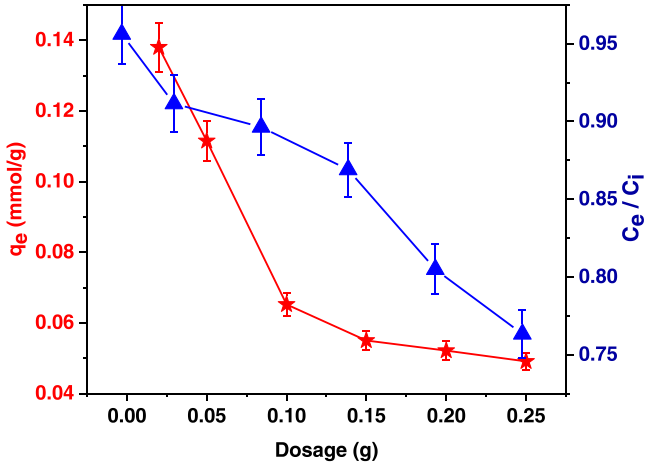

Figure 5. Mesoporous silica nanosphere dosage effect on DOX adsorption.

little to no interaction between the molecules that are adsorbed.[38−41] Based on the surface-supporting sites with varying affinities or the adsorption of heterogeneous surfaces, an empirical equation known as the Freundlich model is developed. The stronger binding sites are thought to be used initially, and as site occupancy increases, the strength of the binding weakens. A pore-filling process first causes subcritical vapors to adsorb onto micropore materials using the empirical Dubinin−Radushkevich isotherm model. It is used to distinguish between chemical and physical adsorption. The Temkin isotherm is based on the hypothesis that the greatest uniform distribution of bond energy occurs during adsorption and that the heat of adsorption for all molecules in the phase drops linearly as the layer is covered. This is shown in Figure 6.

To characterize the isotherm for the adsorption of DOX into the mesoporous silica nanospheres sorbent, it was determined that the Langmuir isotherm model was the most appropriate one, as seen in Figure 6. The Langmuir models, however, were shown to be the most isotherm fitting. And because the adsorption energy was 17.2 kJ·mol^{-1}, the process was chemisorption (Tables S2 and S3).

Adsorption Kinetics. The rate of molecule contact into the supernatant may have an effect on the physicochemical adsorption, and thus it is important to evaluate and investigate the mechanism of adsorption in terms of kinetic changes. A greater knowledge of the real process is also provided by the kinetic study of adsorption. In fact, monitoring and adjusting the effective parameter with an accurate assessment of the adsorption kinetics will increase the adsorption efficiency (Tables S3 and S4). The experimental data with four chosen models—pseudo-first-order,[42] pseudo-second-order,[43] interarticular diffusion,[44] and Elovich[45]—was modified and analyzed for the current study. Figure 7 displays the kinetic models that were used to analyze the experimental results of DOX adsorption.[46] Because DOX molecules had more interaction with the created and constructed system, the kinetic tests showed that drug adsorption was boosted in Table S4. According to experimental findings that suit kinetics models, the simultaneous increase in the dose of the nanocomposite and the contact duration led to improved DOX adsorption. As shown in Figure 7, the pseudo-second-order kinetic model has also effectively predicted the experimental results when compared to the other kinetic models, and when the same conditions are taken into consideration, a higher level of agreement is shown.[47,48]

Adsorption Thermodynamics. It is crucial to examine how temperature influences adsorption because of practical applications.[49] The adsorption investigations were conducted at five different temperatures, as seen in Figure 8. The small increase in adsorption potential for that conduct from 1.39 to 1.99 mmol·g^{-1} confirms that DOX adsorption onto mesoporous silica nanospheres is endothermic.[50] This finding may be the result of enhanced adsorption abilities brought about by an increase in the colored molecule mobility and rate of DOX molecule diffusion over the mesoporous silica nanospheres adsorbent surface with higher temperature,[51] the equilibrium constant for adsorption. Thermodynamic factors affecting the adsorption of DOX include entropy (ΔS°), enthalpy (ΔH°), and the alterations of Gibbs free energy (ΔG°), via the van't Hoff and Arrhenius equations, were measured and assessed, as displayed in Table S5.

Knowing the ideal temperature at which adsorption is most feasible and spontaneous is crucial in industrial settings and water treatment facilities. Depending on the temperature, DOX can either spontaneously or involuntarily adsorb onto adsorbent surfaces. By utilizing the temperature at which the standard free energy is zero (T_0), followed by the lowest temperature at which the process may be regarded as spontaneous, the temperature range can be anticipated.[52] In this instance, 266.71 K has been calculated as the DOX's zero standard free energy temperature (T_0). The low T_0 values demonstrate that the tested adsorbents can remove DOX even at very low temperatures.

BBD Optimization. Table 2 displays the experimental setup and anticipated outcomes for the elimination of DOX. The

https://doi.org/10.1021/acsomega.3c00829
ACS Omega 2023, 8, 14144−14159

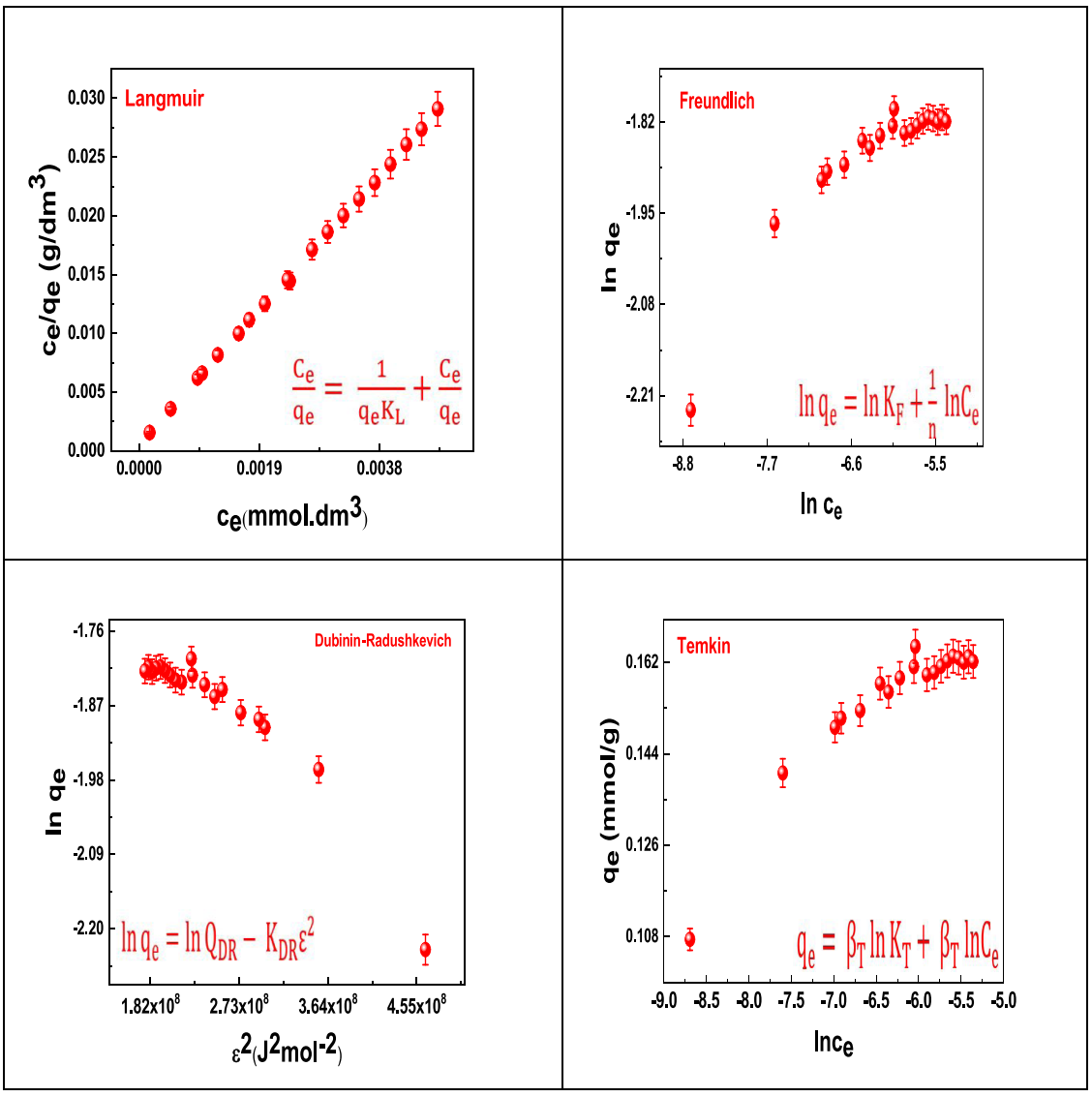

Figure 6. Adsorption isotherm models of adsorption of DOX onto mesoporous silica nanospheres.

following regression equation from a quadratic model showed the link between response and operating parameters.

Coded equation

$$q_e = 1.54649 + 0.04652 \times A + (-0.0363083 \times B) + (-0.0223058 \times C) + 0.139504 \times D + (-0.001375 \times AB) + (-0.000335 \times AC) + 0.01062 \times AD + 0.02362 \times BC + (-0.002505 \times BD) + 0.0304975 \times CD + (-0.0267652 \times A^2) + 0.0623673 \times B^2 + 0.046271 \times C^2 + (-0.0079465 \times D^2)$$

The equation stated in terms of coded factors allows one to predict the reaction for certain concentrations of each ingredient. The high levels of the components are by default expressed a s +1 and the low levels as −1. The coded equation may be used to compare the factor coefficients and estimate the relative weights of the components.

Actual equation

$$q_e = 1.58983 + 0.0223772 \times \text{pH} + (-227.578 \times \text{concentration}) + (-1.69176 \times \text{dose}) + 0.00230783 \times \text{time} + (-0.284818 \times \text{pH} \times \text{concentration}) + (-0.000582609 \times \text{pH} \times \text{dose}) + 4.47158 \times 10^{-5} \times \text{pH} \times \text{time} + 212.724 \times \text{concentration} \times \text{dose} + (-0.0546196 \times \text{concentration} \times \text{time}) + 0.00558307 \times \text{dose} \times \text{time} + (0.00107061 \times \text{pH}^2) + 66899.9 \times \text{concentration}^2 + 3.49875 \times \text{dose}^2 + (-3.52199 \times 10^{-6} \times \text{time}^2)$$

where q_e (mmol/g) is the estimated DOX adsorption capacity and pH (A), concentration (B), dose (C), and time (D), which are the linear terms. A^2, C^2, B^2, and D^2 in this equation also denote quadratic terms, whereas AD, BC, BD, and CD denote interaction terms. The above equation's positive and negative signs represent the parameters' respective antagonistic and

https://doi.org/10.1021/acsomega.3c00829
ACS Omega 2023, 8, 14144−14159

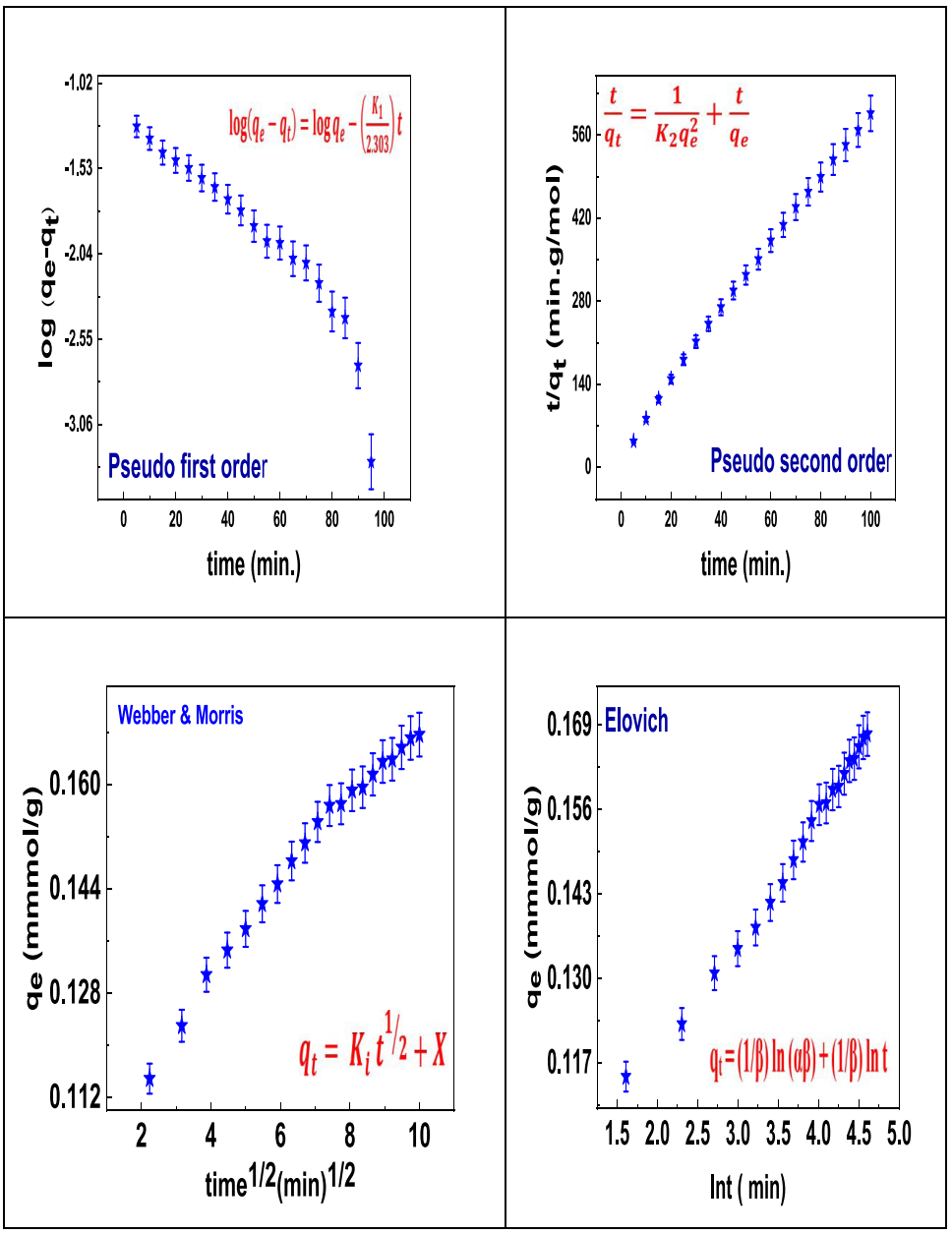

Figure 7. Kinetic isotherm models of adsorption of DOX onto mesoporous silica nanospheres.

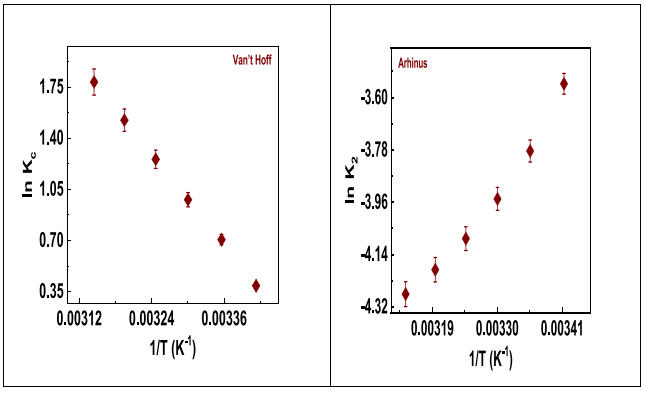

Figure 8. Thermodynamics of DOX adsorption onto mesoporous silica nanospheres.

synergistic effects.Using the equation stated in terms of the actual factors, it is feasible to predict the reaction for certain concentrations of each element. Here, the levels for each component should be stated in their original units. This equation should not be utilized to determine the relative importance of each factor since the coefficients are scaled to take into account the units of each element and the intercept is not at the center of the design space.

The Model *F*-value of 47.61 suggests that the model is significant. As indicated in Table 3, there is just a 0.01% probability that noise could cause an *F*-value this big.

When the *P*-value is less than 0.0500, model terms are deemed significant. In this instance, important model terms were *A*, *B*, *C*, *D*, *CD*, A^2, B^2, and C^2. If the value is higher than 0.1000, the model terms are not significant. If your model contains many extraneous words than those required to maintain hierarchy, model reduction could improve it.

https://doi.org/10.1021/acsomega.3c00829
ACS Omega 2023, 8, 14144−14159

Table 2. Actual DOX Removal Capability from the Experimental Design Matrix with Mesoporous Silica Nanospheres

				removal capacity q_e (mmol/g)	
pH	concentration (mol/L)	dose g/25 mL	time (min)	actual	predicted
2	0.000276	0.135	52.5	1.5496	1.57
7	0.00124153	0.135	52.5	1.54684	1.55
2	0.00124153	0.25	52.5	1.515	1.50
2	0.00124153	0.02	52.5	1.5322	1.54
7	0.00124153	0.25	5	1.3618	1.39
7	0.00124153	0.135	52.5	1.546	1.55
12	0.000276	0.135	52.5	1.6419	1.67
12	0.00124153	0.25	52.5	1.60346	1.59
7	0.000276	0.135	5	1.4907	1.50
7	0.00124153	0.135	52.5	1.546	1.55
7	0.00220706	0.135	5	1.43797	1.43
7	0.00220706	0.135	100	1.71045	1.70
7	0.000276	0.135	100	1.7732	1.78
7	0.000276	0.25	52.5	1.6627	1.65
2	0.00124153	0.135	5	1.3578	1.34
7	0.00124153	0.02	5	1.4727	1.50
7	0.000276	0.02	52.5	1.776	1.74
12	0.00124153	0.02	52.5	1.622	1.64
7	0.00124153	0.135	52.5	1.5468	1.55
7	0.00124153	0.135	52.5	1.5468	1.55
7	0.00124153	0.25	100	1.73089	1.73
12	0.00124153	0.135	100	1.70968	1.71
7	0.00124153	0.02	100	1.7198	1.72
12	0.00124153	0.135	5	1.437	1.41

The lack of fit *F*-value of 3560.60 demonstrates the importance of the misfit. A big lack of fit *F*-value has a noise probability of 0.01%, which is extremely low. The discrepancy is less than 0.2 since the Predicted R^2 of 0.8815 and the Adjusted R^2 of 0.9589 are reasonably in agreement.

Ad_{eq} precision measures the signal-to-noise ratio. The ideal ratio is at least 4. This ratio of 27.389 shows a strong enough signal. To move about the design space, we utilize this model.

The excellent concordance between experimental and anticipated responses is seen in Figure 9a. Remaining is the discrepancy between experimental and anticipated responses. The residual diagrams for DOX removal capability utilizing mesoporous silica nanospheres in various modes are shown in Figure 9b−d (normal plot, residuals *vs* predicted, and residual *vs* run number). In the normal probability plot of Figure 9b, which depicts the typical pattern of the mistakes, the data points form a straight line. In Figure 9c,d, the plots of residuals against run number and residuals against predicted efficiency also illustrate the quadratic model's applicability and the data's random distribution devoid of any trends.

Response Surface Plotting. To assess the impact of each parameter on the response, the anticipated responses were created as 2D contour, cubic, and 3D surface plots, which are displayed in Figure 10. Two essential plot parameters were changed, while the other values remained the same for each plot. The ability to anticipate the DOX removal capacity for different values of the applied parameters can be found by using the contour and surface plots. Figure 10 shows the contour and surface diagrams for DOX elimination percentage as a function of time and dosage (a), initial concentration, and pH (b), as well as the dose and contact time of mesoporous silica nanospheres (c). From Figure 10a, it can be observed that with the increase in time, the adsorption capacity was increased as well, and the adsorbent dose was 0.2 g/25 mL. Based on Figure 10b, higher initial DOX concentration resulted in higher adsorption capacity. With an increase in DOX content, fewer open surface sites on the adsorbent are available, which lowers the adsorption efficiency and raises the adsorption capacity. Finally, from Figure 10c, the adsorption capacity was optimum at 100 min and with an adsorbent dose of 0.02 g/25 mL.

Mechanism of Interaction. Given the chemical makeup of both doxorubicin and silica surfaces, it is possible to hypothesis that the physical interactions between the Si-OH groups of the mesoporous silica nanospheres surface and the $-NH_2$ groups of DOX macromolecules are what primarily cause adsorption. Positively charged $-NH_2$ groups of DOX and ionized Si-OH groups may interact electrostatically. Additionally, leftover unprotonated amine groups contribute to the adsorption process by forming hydrogen bonds with the Si-OH groups of

Table 3. ANOVA for Trials Utilizing Mesoporous Silica Nanospheres to Remove DOX

source	sum of squares	df	mean square	*F*-value	*p*-value	
model	0.3369	14	0.0241	47.61	<0.0001	significant
A—dose	0.0260	1	0.0260	51.38	<0.0001	
B—time	0.0158	1	0.0158	31.30	<0.0001	
C—pH	0.0060	1	0.0060	11.81	0.0040	
D—concentration	0.2335	1	0.2335	462.03	<0.0001	
AB	7.563×10^{-6}	1	7.563×10^{-6}	0.0150	0.9044	
AC	4.489×10^{-7}	1	4.489×10^{-7}	0.0009	0.9766	
AD	0.0005	1	0.0005	0.8925	0.3608	
BC	0.0022	1	0.0022	4.42	0.0542	
BD	0.0000	1	0.0000	0.0497	0.8269	
CD	0.0037	1	0.0037	7.36	0.0168	
A^2	0.0046	1	0.0046	9.19	0.0090	
B^2	0.0252	1	0.0252	49.92	<0.0001	
C^2	0.0139	1	0.0139	27.48	0.0001	
D^2	0.0004	1	0.0004	0.8104	0.3832	
residual	0.0071	14	0.0005			
cor total	0.0071	10	0.0007	3560.60	<0.0001	significant

https://doi.org/10.1021/acsomega.3c00829
ACS Omega 2023, 8, 14144−14159

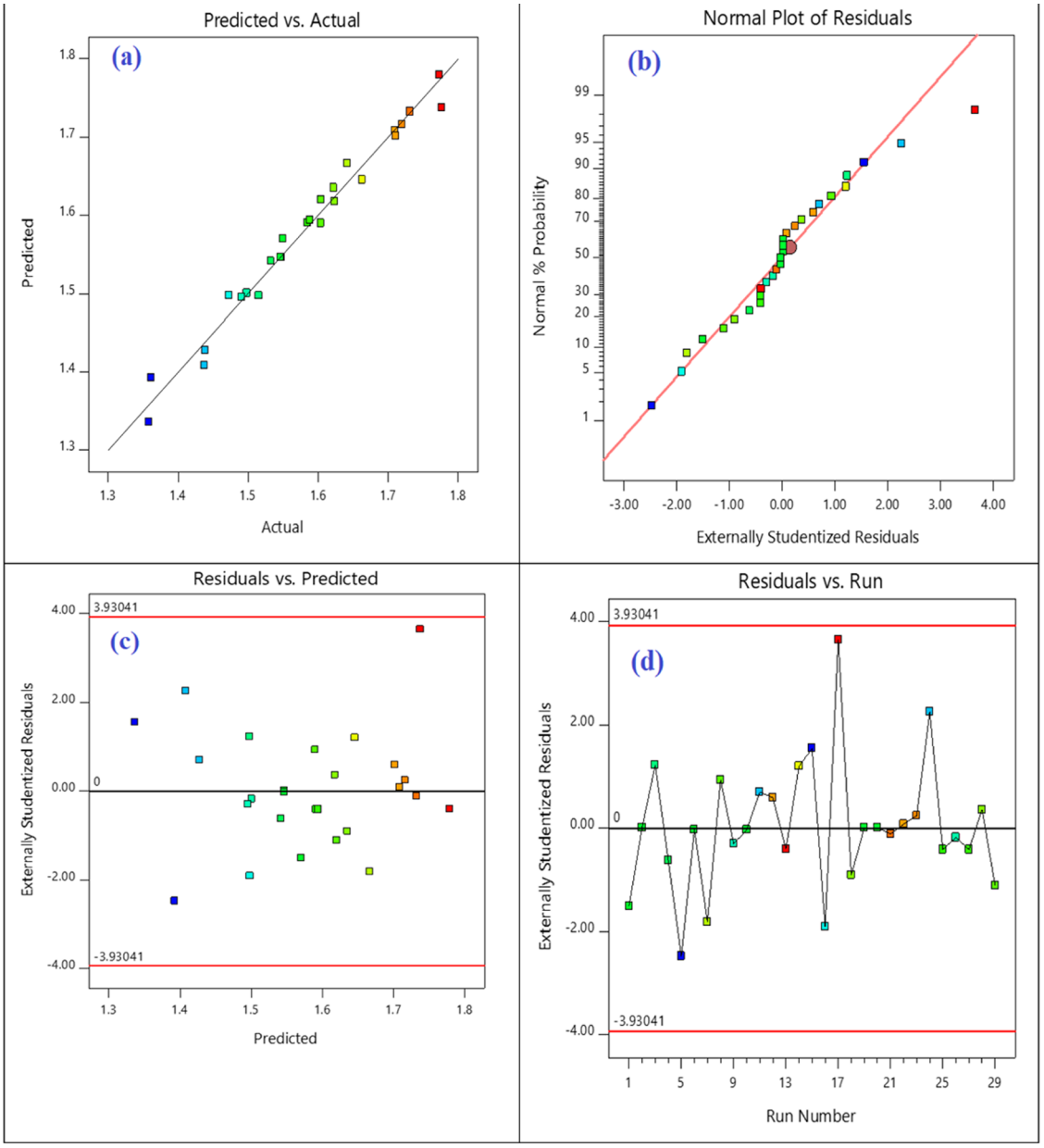

Figure 9. (a) Actual and anticipated values of the fitted model for DOX adsorption are correlated, (b) as are residuals' normal probability plots, (c) externally studentized residuals against expected values, and (d) residuals against the run number.

the mesoporous silica nanospheres.[53] Adsorption is significantly influenced by cooperative forces between DOX molecules, in addition to the direct interactions between DOX and the mesoporous silica nanospheres. DOX is known to have a propensity for self-assembling into higher-order oligomers or dimers in aqueous solutions. The presence of additives, the acidity of the solution, and DOX macromolecule concentration all have a significant impact on how much agglomeration occurs. When aromatic chromophores are arranged in a parallel or antiparallel fashion on the silica surface, it may be hypothesized that additionally, in a solution, the aglycone moieties of DOX stack. The $\pi-\pi$ stacking interactions between adsorbed DOX molecules are to blame for this propensity.[54−57] Therefore, the $\pi-\pi$ interactions and hydrophobic interactions between molecules of DOX that have been adsorbed and those that have been given from solution are what cause DOX polylayers to develop on the silica surface at pH 6.0. Setting the pH to 6 may help with the adsorption process since increasing the ionic strength promotes the self-association of DOX. Maybe sodium ions help the stacking of the chromophores by screening the positively charged DOX molecules or by creating intermolecular interactions. Given the shape of the pore structure of mesoporous silica nanospheres, it is quite likely that DOX polylayers will form, particularly on the external surface of mesoporous silica nanospheres. When adsorbed DOX concentration is substantially lower than what is required for the creation of a monolayer and pH is lowering, polylayer organization does not occur.[58]

Reusability. The capacity of adsorbents to regenerate significantly improves the efficiency of pollutant removal. Mesoporous silica nanospheres used for drug adsorption again after going through regeneration (desorption method) showed excellent removal efficiencies of 97 in the first cycle. The DOX' first cycle clearance efficiencies are discovered to be comparable

https://doi.org/10.1021/acsomega.3c00829
ACS Omega 2023, 8, 14144−14159

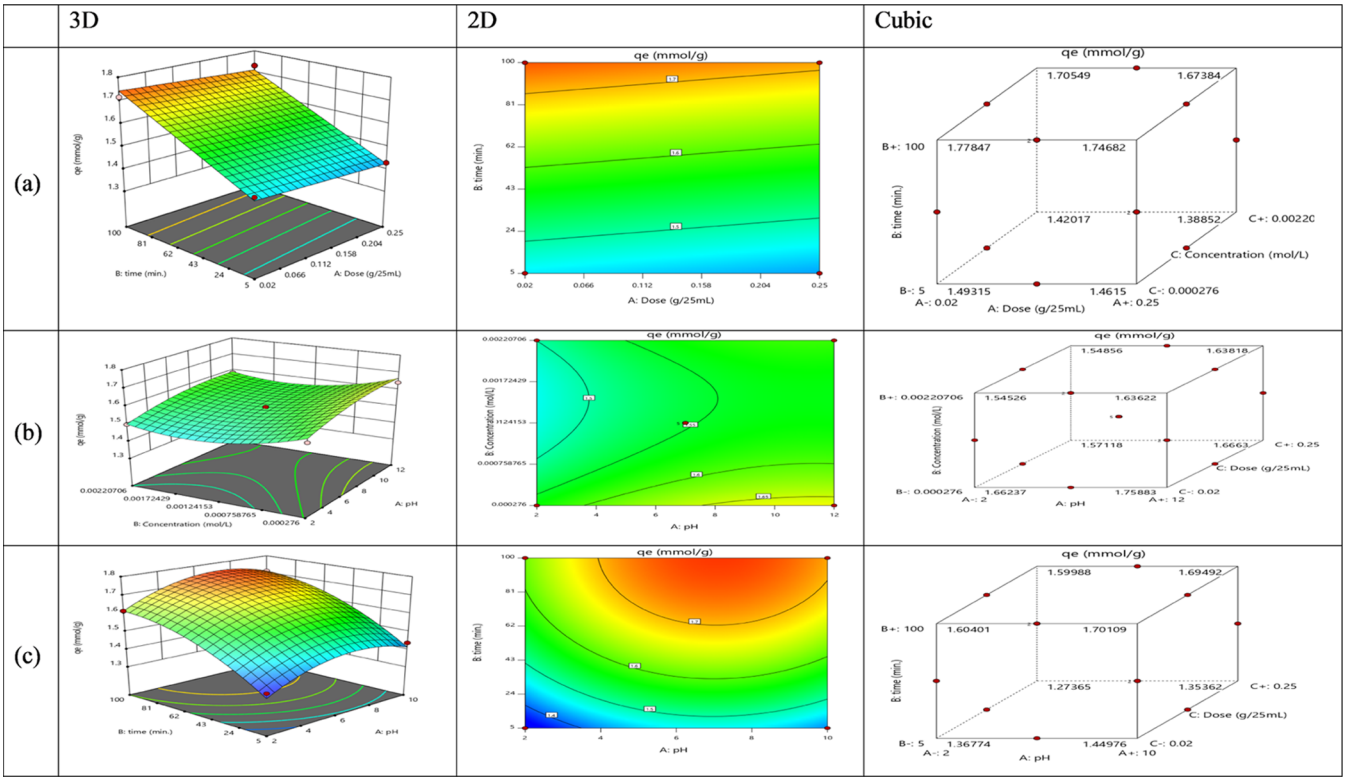

Figure 10. Surface and contour plots for DOX adsorption by mesoporous silica nanospheres.

to those attained with fresh mesoporous silica nanospheres. Following that, three additional cycles demonstrated removal of mesoporous silica nanospheres for the removal of DOX in a decreasing order from 98.6 to 93.2%, which is still a respectable result in the process of removing pharmaceutical contaminants from the aqueous phase.[59] Figure 11 illustrates how the

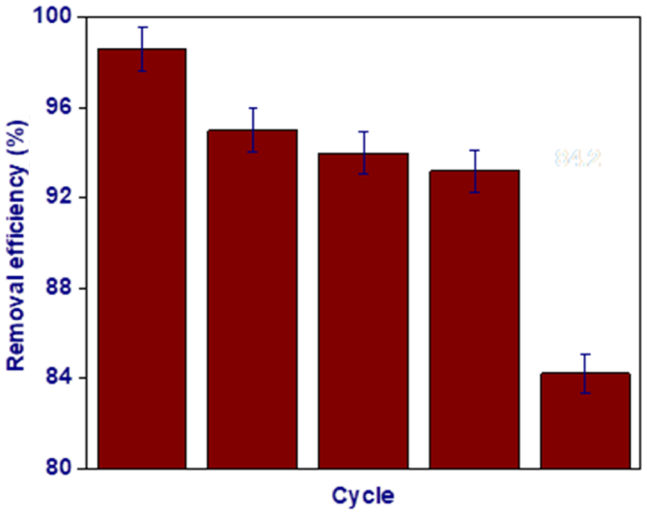

Figure 11. Regeneration efficiency of mesoporous silica nanospheres.

nanocomposites' medication clearance efficacies decreased to 84.2% after four regeneration cycles. The following adsorption and desorption cycles may have caused the surface characteristics of the mesoporous silica nanospheres to degrade, which might account for the decreased efficiency. The functional groups that are present on the mesoporous silica nanospheres would have been exhausted by washing with distilled water. We use water and ethanol in a variety of desorption procedures as well as mechanical forces.[60]

Comparison with Other Adsorbents. Mesoporous silica nanospheres are used as the adsorbent in Table 4 to compare

Table 4. Adsorption of DOX by Various Adsorbents

adsorbent	Q_m (mg/g)	reference
pristine MWCNTs	185.2	[58]
GO@Fe_3O_4@MSNP@CS	390	[60]
MSAC	135.89	[61]
Zr-MOF	646.78	[52]
GO	909	[63]
Fe_3O_4@ZIF-8	804.84	[64]
mesoporous silica nanospheres	1021	this work

and contrast the best DOX adsorption power with the other adsorbents described before.[58,60−64] It is obvious that our adsorbent mesoporous silica nanosphere adsorption has a significantly high absorption capacity compared to the other adsorbents.

Application of Real Samples. To evaluate the performance of the composite made of mesoporous silica nanospheres, two samples of industrial waste were supplied. These two samples were from Ismailia's industrial zone. We discovered that a sizable amount of the paint industry's industrial drainage sample had mixed debris made up of polishing glaze colors and tile. As a result, the samples were given 48 h to settle before the dust was eliminated using a filter made of many layers of linen. The substance was once more sedimented after 48 h. The filter paper was used to remove the ultrafine dust residue, which exposed a bright blue color with a blank absorption of 302 nm. Filtration and sample preparation were finished. Under optimal conditions, the adsorption of the DOX was investigated. 64.2

https://doi.org/10.1021/acsomega.3c00829
ACS Omega 2023, 8, 14144−14159

and 96.8%, respectively, of the dye was absorbed. According to the study's findings, it is possible to effectively remove colors from industrial effluent resources by employing mesoporous silica nanospheres.

CONCLUSIONS

In this work, novel mesoporous silica nanospheres were successfully synthesized, characterized, and applied for the removal of DOX. The results demonstrate that mesoporous silica nanospheres are an effective and high-performance adsorbent for DOX removal. The ideal experimental settings for increased DOX elimination were found using the Box–Behnken design and response surface methods. Four different factors, including solution pH, DOX concentration, dose, and time, were used in the optimization. Mesoporous silica nanospheres have been described as having unique characteristics and a great deal of potential as an adsorbent. This research also showed that various surface morphologies, functional groupings, and huge surface regions are important characterization elements. The Langmuir model was used to calculate the q_m for DOX of the mesoporous silica nanospheres since it best matched the experimental outcomes. This value was 1.88 mmol·g^{-1}. The kinetic investigation further showed that interparticle diffusion was not the main mechanism driving the adsorption of DOX on mesoporous silica nanospheres, and the experimental kinetic results confirmed the PSO model. In addition, the following environmental conditions were excellent for attaining the maximum DOX: shaking speed = 200 rpm; t = 100 min; dose = 0.02 g; and pH = 6. Mesoporous silica nanospheres had been recycled five times with high efficiency.

ASSOCIATED CONTENT

Supporting Information

The Supporting Information is available free of charge at https://pubs.acs.org/doi/10.1021/acsomega.3c00829.

Detailed procedure for the materials, synthesis of mesoporous silica nanospheres, instruments, removal and batch studies of the mesoporous silica nanospheres, adsorption isotherm, and adsorption kinetics and thermodynamics (PDF)

AUTHOR INFORMATION

Corresponding Author

Ahmed Shahat − *Department of Chemistry, Faculty of Science, Suez University, Suez 8151650, Egypt;* orcid.org/0000-0001-9198-9712; Email: ashahat@aucegypt.edu

Authors

Khalid Althumayri − *Department of Chemistry, College of Science, Taibah University, 30002 Al-Madinah Al-Munawarah, Saudi Arabia*

Ahlem Guesmi − *Chemistry Department, College of Science, IMSIU (Imam Mohammad Ibn Saud Islamic University), Riyadh 11432, Saudi Arabia;* orcid.org/0000-0002-7552-4146

Wesam Abd El-Fattah − *Chemistry Department, College of Science, IMSIU (Imam Mohammad Ibn Saud Islamic University), Riyadh 11432, Saudi Arabia; Department of Chemistry, Faculty of Science, Port Said University, Port Said 43518, Egypt;* orcid.org/0000-0002-1083-7694

Lotfi Khezami − *Chemistry Department, College of Science, IMSIU (Imam Mohammad Ibn Saud Islamic University), Riyadh 11432, Saudi Arabia*

Taoufik Soltani − *Physics Laboratory of Soft Matter and Electromagnetic Modelling, Faculty of Sciences of Tunis, University of Tunis El Manar, Tunis 1068, Tunisia*

Naoufel Ben Hamadi − *Chemistry Department, College of Science, IMSIU (Imam Mohammad Ibn Saud Islamic University), Riyadh 11432, Saudi Arabia; Laboratory of Heterocyclic Chemistry, Natural Products and Reactivity (LR11ES39), Faculty of Science of Monastir, UM (University of Monastir), Monastir 5019, Tunisia;* orcid.org/0000-0002-2410-5275

Complete contact information is available at: https://pubs.acs.org/10.1021/acsomega.3c00829

Notes

The authors declare no competing financial interest.

ACKNOWLEDGMENTS

The authors extend their appreciation to the Deanship of Scientific Research at Imam Mohammad Ibn Saud Islamic University (IMSIU) for funding and supporting this work through Research Partnership Program No. RP-21-09-71.

REFERENCES

(1) (a) Awual, M. R. Mesoporous composite material for efficient lead(II) detection and removal from aqueous media. *J. Environ. Chem. Eng.* **2019**, *7*, No. 103124. (b) Awual, M. R. A facile composite material for enhanced cadmium(II) ion capturing from wastewater. *J. Environ. Chem. Eng.* **2019**, *7*, No. 103378. (c) Hasan, M. M. A ligand based innovative composite material for selective lead(II) capturing from wastewater. *J. Mol. Liq.* **2019**, *294*, No. 111679. (d) Awual, M. R.; Asiri, A. M.; Rahman, M. M.; Alharthi, N. H. Assessment of enhanced nitrite removal and monitoring using ligand modified stable conjugate materials. *Chem. Eng. J.* **2019**, *363*, 64–72. (e) Awual, M. R.; Islam, A.; Hasan, M. M.; Rahman, M. M.; Asiri, A. M.; Khaleque, M. A.; Sheikh, M. C. Introducing an alternate conjugated material for enhanced lead(II) capturing from wastewater. *J. Clean. Prod.* **2019**, *224*, 920–929.

(2) (a) Awual, M. R.; Hasan, M. M.; Islam, A.; Rahman, M. M.; Asiri, A. M.; Khaleque, M. A.; Sheikh, M. C. Introducing an amine functionalized novel conjugate material for toxic nitrite detection and adsorption from wastewater. *J. Clean. Prod.* **2019**, *228*, 778–785. (b) Awual, M. R. Assessing of lead(II) capturing from contaminated wastewater using ligand doped conjugate adsorbent. *Chem. Eng. J.* **2016**, *289*, 65–73. (c) Awual, M. R. Ring size dependent crown ether based mesoporous adsorbent for high cesium adsorption from wastewater. *Chem. Eng. J.* **2016**, *303*, 539–546. (d) Awual, M. R.; Hasan, M. M.; Islam, A.; Rahman, M. M.; Asiri, A. M.; Khaleque, M. A.; Sheikh, M. C. Offering an innovative composited material for effective lead(II) monitoring and removal from polluted water. *J. Clean. Prod.* **2019**, *231*, 214–223. (e) Awual, M. R.; Khraisheh, M.; Alharthi, N. H.; Luqman, M.; Islam, A.; Karim, M. R.; Rezaul Karim, M.; Rahman, M. M.; Khaleque, M. A. Efficient detection and adsorption of cadmium(II) ions using innovative nano-composite materials. *Chem. Eng. J.* **2018**, *343*, 118–127.

(3) (a) Awual, M. R.; Alharthi, N. H.; Hasan, M. M.; Karim, M. R.; Islam, A.; Znad, H.; Hossain, M. A.; Halim, M. E.; Rahman, M. M.; Khaleque, M. A. Inorganic-organic based novel nano-conjugate material for effective cobalt(II) ions capturing from wastewater. *Chem. Eng. J.* **2017**, *324*, 130–139. (b) Awual, M. R. Efficient phosphate removal from water for controlling eutrophication using novel composite adsorbent. *J. Clean. Prod.* **2019**, *228*, 1311–1319. (c) Awual, M. R. Novel ligand functionalized composite material for efficient copper(II) capturing from wastewater sample. *Compos. B Eng.*

2019, *172*, 387−396. (d) Awual, M. R.; Hasan, M. M.; Rahman, M. M.; Asiri, A. M. Novel composite material for selective copper(II) detection and removal from aqueous media. *J. Mol. Liq.* **2019**, *283*, 772−780. (e) Awual, M. R.; Hasan, M. M.; Asiri, A. M.; Rahman, M. M. Cleaning the arsenic(V) contaminated water for safe-guarding the public health using novel composite material. *Compos. B Eng.* **2019**, *171*, 294−301.

(4) (a) Awual, M. R.; Hasan, M. M.; Eldesoky, G. E.; Khaleque, M. A.; Rahman, M. M.; Naushad, M. Facile mercury detection and removal from aqueous media involving ligand impregnated conjugate nanomaterials. *Chem. Eng. J.* **2016**, *290*, 243−251. (b) Awual, M. R. Innovative composite material for efficient and highly selective Pb(II) ion capturing from wastewater. *J. Mol. Liq.* **2019**, *284*, 502−510. (c) Awual, M. R. Novel conjugated hybrid material for efficient lead(II) capturing from contaminated wastewater. *Mater. Sci. Eng. C* **2019**, *101*, 686−695. (d) Awual, M. R.; Hasan, M. M.; Khaleque, M. A.; Shiekh, M. C. Treatment of copper(II) containing wastewater by a newly developed ligand based facial conjugate materials. *Chem. Eng. J.* **2016**, *288*, 368−376. (e) Awual, M. R.; Miyazaki, M.; Miyazaki, Y.; Taguchi, T.; Shiwaku, H.; Yaita, T. Encapsulation of cesium from contaminated water with highly selective facial organic-inorganic mesoporous hybrid adsorbent. *Chem. Eng. J.* **2016**, *291*, 128−137.

(5) (a) Awual, M. R. A novel facial composite adsorbent for enhanced copper(II) detection and removal from wastewater. *Chem. Eng. J.* **2015**, *266*, 368−375. (b) Hasan, M. M.; Iqbal, J.; Islam, A.; Islam, M. A.; Khandaker, S.; Asiri, A. M.; Rahman, M. M. Ligand based sustainable composite material for sensitive nickel(II) capturing in aqueous media. *J. Environ. Chem. Eng.* **2020**, *8*, No. 103591. (c) Hasan, M. M.; Islam, A.; Asiri, A. M.; Rahman, M. M. Optimization of an innovative composited material for effective monitoring and removal of cobalt(II) from wastewater. *J. Mol. Liq.* **2020**, *298*, No. 112035. (d) Awual, M. R. An efficient composite material for selective lead(II) monitoring and removal from wastewater. *J. Environ. Chem. Eng.* **2019**, *7*, No. 103087. (e) Awual, M. R.; Hasan, M. M.; Asiri, A. M.; Rahman, M. M. Novel optical composite material for efficient vanadium(III) capturing from wastewater. *J. Mol. Liq.* **2019**, *283*, 704−712.

(6) Sílvio, V., Jr. *Analytical Chemistry Applied to Emerging Pollutants*; Springer International Publishing.

(7) Arjmand, O.; Ardjmand, M.; Amani, A. M.; Eikani, M. H. Effective Adsorption of Doxorubicin Hydrochloride on Green Magnetic/Graphene Oxide/Chitosan/Allium Sativum/Quercus/NanoComposite. *J. Acta Chimica Slovenica* **2020**, *67*, 496−506.

(8) Liu, J.; Cui, L.; Losic, D. Graphene and graphene oxide as new nanocarriers for drug delivery applications. *Acta Biomaterialia* **2013**, *9*, 9243−9257.

(9) Xi, Z.; Wei, K.; Wang, Q.; Kim, M. J.; Sun, S.; Fung, V.; Xia, X. Nickel−Platinum Nanoparticles as Peroxidase Mimics with a Record High Catalytic Efficiency. *J. Am. Chem. Soc.* **2021**, *143*, 2660−2664.

(10) Bi, D.; Zhao, L.; Yu, R.; Li, H.; Guo, Y.; Wang, X.; Han, M. Surface modification of doxorubicin-loaded nanoparticles based on polydopamine with pH-sensitive property for tumor targeting therapy. *J. Drug Delivery* **2018**, *25*, 564−575.

(11) Cai, W.; Guo, M.; Weng, X.; Zhang, W.; Chen, Z. Adsorption of doxorubicin hydrochloride on glutaric anhydride functionalized Fe_3O_4@ SiO2 magnetic nanoparticles. *J. Mater. Sci. Eng.: C* **2019**, *98*, 65−73.

(12) (a) Awual, M. R. Solid phase sensitive palladium(II) ions detection and recovery using ligand based efficient conjugate nanomaterials. *Chem. Eng. J.* **2016**, *300*, 264−272. (b) Abbas, K.; Znad, H.; Awual, M. R. A ligand anchored conjugate adsorbent for effective mercury(II) detection and removal from aqueous media. *Chem. Eng. J.* **2018**, *334*, 432−443. (c) Awual, M. R.; Hasan, M. M. Fine-tuning mesoporous adsorbent for simultaneous ultra-trace palladium(II) detection, separation and recovery. *J. Ind. Eng. Chem.* **2015**, *21*, 507−515. (d) Awual, M. R.; Hasan, M. M. Colorimetric detection and removal of copper(II) ions from wastewater samples using tailor-made composite adsorbent. *Sens. Actuators, B* **2015**, *206*, 692−700. (e) Awual, M. R.; Eldesoky, G. E.; Yaita, T.; Naushad, M.; Shiwaku, H.; AlOthman, Z. A.; Suzuki, S. Schiff based ligand containing nano-composite adsorbent for optical copper(II) ions removal from aqueous solutions. *Chem. Eng. J.* **2015**, *279*, 639−647.

(13) (a) Awual, M. R. Investigation of potential conjugate adsorbent for efficient ultra−trace gold(III) detection and recovery. *J. Ind. Eng. Chem.* **2014**, *20*, 3493−3501. (b) Awual, M. R.; Hasan, M. M. Novel conjugate adsorbent for visual detection and removal of toxic lead(II) ions from water. *Micropor. Mesopor. Mater.* **2014**, *196*, 261−269. (c) Awual, M. R.; Ismael, M.; Khaleque, M. A.; Yaita, T. Ultra-trace copper(II) detection and removal from wastewater using novel meso-adsorbent. *J. Ind. Eng. Chem.* **2014**, *20*, 2332−2340. (d) Yaita, T.; Kobayashi, T.; Shiwaku, H.; Suzuki, S. Improving cesium removal to clean-up the contaminated water using modified conjugate material. *J. Environ. Chem. Eng.* **2020**, *8*, No. 103684. (e) Hasan, M. M.; Iqbal, J.; Islam, A.; Islam, M. A.; Asiri, A. M.; Rahman, M. M. Naked-eye lead(II) capturing from contaminated water using innovative large-pore facial composite materials. *Microchem. J.* **2020**, *154*, No. 104585.

(14) (a) Awual, M. R. New type mesoporous conjugate material for selective optical copper(II) ions monitoring & removal from polluted waters. *Chem. Eng. J.* **2017**, *307*, 85−94. (b) Awual, M. R.; Alharthi, N. H.; Okamoto, Y.; Karim, M. R.; Halim, M. E.; Hasan, M. M.; Rahman, M. M.; Islam, M. M.; Khaleque, M. A.; Sheikh, M. C. Ligand field effect for Dysprosium(III) and Lutetium(III) adsorption and EXAFS coordination with novel composite nanomaterials. *Chem. Eng. J.* **2017**, *320*, 427−435. (c) Awual, M. R.; Yaita, T.; Shiwaku, H.; Suzuki, S. A sensitive ligand embedded nano-conjugate adsorbent for effective cobalt(II) ions capturing from contaminated water. *Chem. Eng. J.* **2015**, *276*, 1−10. (d) Awual, M. R.; Yaita, T.; Suzuki, S.; Shiwaku, H. Ultimate selenium(IV) monitoring and removal from water using a new class of organic ligand based composite adsorbent. *J. Hazard. Mater.* **2015**, *291*, 111−119. (e) Awual, M. R. Novel nanocomposite materials for efficient and selective mercury ions capturing from wastewater. *Chem. Eng. J.* **2017**, *307*, 456−465.

(15) (a) Awual, M. R.; Hasan, M. M.; Shahat, A.; Naushad, M.; Shiwaku, H.; Yaita, T. Investigation of ligand immobilized nano-composite adsorbent for efficient cerium(III) detection and recovery. *Chem. Eng. J.* **2015**, *265*, 210−218. (b) Awual, M. R.; Hasan, M. M.; Khaleque, M. A. Efficient selenium(IV) detection and removal from water by tailor-made novel conjugate adsorbent. *Sens. Actuators, B* **2015**, *209*, 194−202. (c) Awual, M. R.; Rahman, I.M.M.; Yaita, T.; Khaleque, M. A.; Ferdows, M. pH dependent Cu(II) and Pd(II) ions detection and removal from aqueous media by an efficient mesoporous adsorbent. *Chem. Eng. J.* **2014**, *236*, 100−109. (d) Awual, M. R.; Yaita, T. Rapid sensing and recovery of palladium(II) using N,N-bis-(salicylidene)1,2-bis(2-aminophenylthio)ethane modified sensor ensemble adsorbent. *Sens. Actuators, B* **2013**, *183*, 332−341. (e) Awual, M. R.; Yaita, T.; Shiwaku, H. Design a novel optical adsorbent for simultaneous ultra-trace cerium(III) detection, sorption and recovery. *Chem. Eng. J.* **2013**, *228*, 327−335.

(16) (a) Kobayashi, T.; Miyazaki, Y.; Motokawa, R.; Shiwaku, H.; Suzuki, S.; Okamoto, Y.; Yaita, T. Selective lanthanide sorption and mechanism using novel hybrid Lewis base (N−methyl−N-phenyl−1,10−phenanthroline−2−carboxamide) ligand modified adsorbent. *J. Hazard. Mater.* **2013**, *252*−*253*, 313−320. (b) Awual, M. R.; Jyo, A.; Ihara, T.; Seko, N.; Seko, N.; Tamada, M.; Lim, K. T. Enhanced trace phosphate removal from water by zirconium(IV) loaded fibrous adsorbent. *Water Res.* **2011**, *45*, 4592−4600. (c) Hasan, M. M.; Hasan, M. N.; Islam, M. M.; Shenashen, M. A.; Iqbal, J. Biodegradable natural carbohydrate polymeric sustainable adsorbents for efficient toxic dye removal from wastewater. *J. Mol. Liq.* **2020**, *319*, No. 114356. (d) Hasan, M. N.; Shenashen, M. A.; Hasan, M. M.; Znad, H.; Awual, M. R. Assessing of cesium removal from wastewater using functionalized wood cellulosic adsorbent. *Chemosphere* **2021**, *270*, No. 128668. (e) Awual, M. R.; Kobayashi, T.; Shiwaku, H.; Miyazaki, Y.; Motokawa, R.; Suzuki, S.; Okamoto, Y.; Yaita, T. Evaluation of lanthanide sorption and their coordination mechanism by EXAFS measurement using novel hybrid adsorbent. *Chem. Eng. J.* **2013**, *225*, 558−566.

(17) (a) Awual, M. R.; Ismael, M.; Yaita, T.; El-Safty, S. A.; Shiwaku, H.; Okamoto, Y.; Suzuki, S. Trace copper(II) ions detection and

https://doi.org/10.1021/acsomega.3c00829
ACS Omega 2023, 8, 14144−14159

removal from water using novel ligand modified composite adsorbent. *Chem. Eng. J.* **2013**, *222*, 67−76. (b) Awual, M. R.; Yaita, T.; El-Safty, S. A.; Shiwaku, H.; Okamoto, Y.; Suzuki, S. Investigation of palladium(II) detection and recovery using ligand modified conjugate adsorbent. *Chem. Eng. J.* **2013**, *222*, 172−179. (c) Hasan, M. N.; Salman, M. S.; Islam, A.; Znad, H.; Hasan, M. M. Sustainable composite sensor material for optical cadmium(II) monitoring and capturing from wastewater. *Microchem. J.* **2021**, *161*, No. 105800. (d) Hasan, M. M.; Shenashen, M. A.; Hasan, M. N.; Znad, H.; Salman, M. S.; Awual, M. R. Natural biodegradable polymeric bioadsorbents for efficient cationic dye encapsulation from wastewater. *J. Mol. Liq.* **2021**, *323*, No. 114587. (e) Hassan, H. M.; Shahat, A.; Azzazy, H. M. E.; Abd El-aal, R. M.; El-Sayed, W. N.; Elwahed, A. A.; Awual, M. R. A novel and potential chemical sensor for effective monitoring of Fe(II) ion in corrosion systems of water samples. *Microchem. J.* **2020**, *154*, No. 104578.

(18) Zhu, S.; Chang, C.; Sun, Y.; Duan, G.; Chen, Y.; Pan, J.; Tang, Y.; Wan, P. Modification of stainless steel fiber felt via in situ self-growth by electrochemical induction as a robust catalysis electrode for oxygen evolution reaction. *J. Int. J. Hydrogen Energy* **2020**, *45*, 1810−1821.

(19) Di Renzo, F.; Testa, F.; Chen, J. D.; Cambon, H.; Galarneau, A.; Plee, D.; Fajula, F. Micropor. *Mesopor. Mater.* **1999**, *28*, 437.

(20) Shahat, A.; Trupp, S. J. S. Sensitive, selective, and rapid method for optical recognition of ultra-traces level of Hg (II), Ag (I), Au (III), and Pd (II) in electronic wastes. *Sens. Actuators, B* **2017**, *245*, 789−802.

(21) (a) El-Safty, S. A.; Shahat, A.; Rabiul Awual, M. Efficient adsorbents of nanoporous aluminosilicate monoliths for organic dyes from aqueous solution. *J. Colloid Interface Sci.* **2011**, *359*, 9−18. (b) Alam, M. M.; Uddin, M. T.; Asiri, A. M.; Fazal, M. A.; Islam, M. A.; et al. Fabrication of selective L-glutamic acid sensor in electrochemical technique from wet-chemically prepared RuO2 doped ZnO nanoparticles. *Mater. Chem. Phys.* **2020**, *251*, No. 123029. (c) Alam, M. M.; Asiri, A. M.; Uddin, M. T.; Islam, M. A.; et al. One-step wet-chemical synthesis of ternary ZnO/CuO/Co3O4 nanoparticles for sensitive and selective melamine sensor development. *New J. Chem.* **2019**, *43*, 4849−4858. (d) Uddin, M. T.; Asiri, A. M.; Rahman, M. M.; et al. Detection of uric acid based on doped $ZnO/Ag_2O/Co_3O_4$ nanoparticle loaded glassy carbon electrode. *New J. Chem.* **2019**, *43*, 8651−8659.

(22) Kim, T.-W.; Chung, P.-W.; Lin, V.S.-Y. Facile synthesis of monodisperse spherical MCM-48 mesoporous silica nanoparticles with controlled particle size. *Chem. Mater.* **2010**, *22*, 5093−5104.

(23) El-Safty, S.; Shahat, A.; Awual, M. R.; Mekawy, M. Large three-dimensional mesocage pores tailoring silica nanotubes as membrane filters: nanofiltration and permeation flux of proteins. *J. Mater. Chem.* **2011**, *21*, 5593−5603.

(24) Du, X.; He, J. Fine-tuning of silica nanosphere structure by simple regulation of the volume ratio of cosolvents. *J Langmuir* **2010**, *26*, 10057−10062.

(25) Gu, F. N.; Lin, W. G.; Yang, J. Y.; Wei, F.; Wang, Y.; Zhu, J. H. Fabrication of centimeter-sized sphere of mesoporous silica with well-defined hollow nanosphere topology and its high performance in adsorbing phenylalanine. *J Microporous Mesoporous Mater.* **2012**, *151*, 142−148.

(26) P. N., Kioni; Y., Gao; Z., Tang; E., Gatebe; H., Wanyika, Synthesis and characterization of ordered mesoporous silica nanoparticles with tunable physical properties by varying molar composition of reagents, (2011).

(27) Guo, X.; Deng, Y.; Tu, B.; Zhao, D. Facile synthesis of hierarchically mesoporous silica particles with controllable cavity in their surfaces. *Langmuir* **2010**, *26*, 702−708.

(28) (a) Awual, M. R.; Suzuki, S.; Suzuki, S.; Taguchi, T.; Taguchi, T.; Shiwaku, H.; Shiwaku, H.; Okamoto, Y.; Okamoto, Y.; Yaita, T. Radioactive cesium removal from nuclear wastewater by novel inorganic and conjugate adsorbents. *Chem. Eng. J.* **2014**, *242*, 127−135. (b) Awual, M. R.; Yaita, T.; Yaita, T.; El-Safty, S. A.; El-Safty, S. A.; Shiwaku, H.; Shiwaku, H.; Suzuki, S.; Suzuki, S.; Okamoto, Y. Copper(II) ions capturing from water using ligand modified a new type mesoporous adsorbent. *Chem. Eng. J.* **2013**, *221*, 322−330. (c) Rabiul Awual, M.; Hasan, M. M.; Munjur Hasan, M.; Ihara, T.; Ihara, T.; Yaita, T. Mesoporous silica based novel conjugate adsorbent for efficient selenium(IV) detection and removal from water. *Micropor. Mesopor. Mater.* **2014**, *197*, 331−338. (d) Awual, M. R.; Yaita, T.; Taguchi, T.; Shiwaku, H.; Suzuki, S.; Okamoto, Y. Selective cesium removal from radioactive liquid waste by crown ether immobilized new class conjugate adsorbent. *J. Hazard. Mater.* **2014**, *278*, 227−235. (e) Islam, A.; Roy, S.; Khan, M. A.; Mondal, P.; Teo, S. H.; Taufiq-Yap, Y. H.; Ahmed, M. T.; Choudhury, T. R.; Abdulkreem-Alsultan, G.; Alsultan, G. A.; Khandaker, S. Improving valuable metal ions capturing from spent Li-ion batteries with novel materials and approaches. *J. Mol. Liq.* **2021**, *338*, No. 116703.

(29) (a) Awual, M. R.; Hasan, M. M. A novel fine-tuning mesoporous adsorbent for simultaneous lead(II) detection and removal from wastewater. *Sens. Actuators, B* **2014**, *202*, 395−403. (b) Awual, M. R.; Hasan, M. M.; Shahat, A. Functionalized novel mesoporous adsorbent for selective lead(II) ions monitoring and removal from wastewater. *Sens. Actuators, B* **2014**, *203*, 854−863. (c) Islam, A.; Ahmed, T.; Awual, M. R.; Rahman, A.; Sultana, M.; Aziz, A. A.; Monir, M. U.; Teo, S. H.; Hasan, M. Advances in sustainable approaches to recover metals from e-waste-A review. *J. Clean. Prod.* **2020**, *244*, No. 118815. (d) Islam, A.; Teo, S. H.; Awual, M. R.; Taufiq-Yap, Y. H. Assessment of clean H_2 energy production from water using novel silicon photocatalyst. *J. Clean. Prod.* **2020**, *244*, No. 118805. (e) Islam, M. A.; Angove, M. J.; Morton, D. W.; Pramanik, B. K.; Awual, M. R. A mechanistic approach of chromium(VI) adsorption onto manganese oxides and boehmite. *J. Environ. Chem. Eng.* **2020**, *8*, No. 103515.

(30) (a) Awual, M. R.; Hasan, M. M.; Znad, H. Organic-inorganic based nano-conjugate adsorbent for selective palladium(II) detection, separation and recovery. *Chem. Eng. J.* **2015**, *259*, 611−619. (b) Awual, M. R.; Hasan, M. M.; Naushad, M.; Shiwaku, H.; Yaita, T. Preparation of new class composite adsorbent for enhanced palladium(II) detection and recovery. *Sens. Actuators, B* **2015**, *209*, 790−797. (c) Islam, M. A.; Awual, M. R.; Angove, M. J. A review on nickel(II) adsorption in single and binary component systems and future path. *J. Environ. Chem. Eng.* **2019**, *7*, No. 103305. (d) Islam, A.; Teo, S. H.; Awual, M. R.; Taufiq-Yap, Y. H. Improving the hydrogen production from water over MgO promoted Ni-Si/CNTs photocatalyst. *J. Clean. Prod.* **2019**, *238*, No. 117887. (e) Kamel, R. M.; Shahat, A.; Hegazy, W. H.; Khodier, E. M.; Awual, M. R. Efficient toxic nitrite monitoring and removal from aqueous media with ligand based conjugate materials. *J. Mol. Liq.* **2019**, *285*, 20−26.

(31) (a) Awual, M. R.; Khaleque, M. A.; Ratna, Y.; Znad, H. Simultaneous ultra-trace palladium(II) detection and recovery from wastewater using new class meso-adsorbent. *J. Ind. Eng. Chem.* **2015**, *21*, 405−413. (b) Khandaker, S.; Chowdhury, M. F.; Awual, M. R.; Islam, A.; Kuba, T. Efficient cesium encapsulation from contaminated water by cellulosic biomass based activated wood charcoal. *Chemosphere* **2021**, *262*, No. 127801. (c) Khandaker, S.; Toyohara, Y.; Saha, G. C.; Awual, M. R.; Kuba, T. Development of synthetic zeolites from bio-slag for cesium adsorption: kinetic, isotherm and thermodynamic studies. *J. Water Process Eng.* **2020**, *33*, No. 101055. (d) Kubra, K. T.; Salman, M. S.; Hasan, M. N. Enhanced toxic dye removal from wastewater using biodegradable polymeric natural adsorbent. *J. Mol. Liq.* **2021**, *328*, No. 115468. (e) Mazrouaa, A. M.; Mansour, N. A.; Abed, M. Y.; Youssif, M. A.; Shenashen, M. A.; Awual, M. R. Nano-composite multi-wall carbon nanotubes using poly(pphenylene terephthalamide) for enhanced electric conductivity. *J. Environ. Chem. Eng.* **2019**, *7*, No. 103002.

(32) (a) Naushad, M.; Alqadami, A. A.; Al-Kahtani, A. A.; Ahamad, T.; Awual, M. R.; Tatarchuk, T. Adsorption of textile dye using para-aminobenzoic acid modified activated carbon: Kinetic and equilibrium studies. *J. Mol. Liq.* **2019**, *296*, No. 112075. (b) Kubra, K. T.; Salman, M. S.; Znad, H.; Hasan, M. N. Efficient encapsulation of toxic dye from wastewater using biodegradable polymeric adsorbent. *J. Mol. Liq.* **2021**, *329*, No. 115541. (c) Kubra, K. T.; Salman, M. S.; Hasan, M. N.; Islam, A.; Teo, S. H.; Hasan, M. M.; Sheikh, M. C.; Awual, M. R. Sustainable detection and capturing of cerium(III) using ligand embedded solid-state conjugate adsorbent. *J. Mol. Liq.* **2021**, *338*, No. 116667. (d) Salman, M. S.; Znad, H.; Hasan, M. N.; Hasan, M. M. Optimization of innovative composite sensor for Pb(II) detection and capturing from

https://doi.org/10.1021/acsomega.3c00829
ACS Omega 2023, 8, 14144−14159

water samples. *Microchem. J.* **2021**, *160*, No. 105765. (e) Shahat, A.; Kubra, K. T.; Salman, M. S.; Hasan, M. N.; Hasan, M. M. Novel solid-state sensor material for efficient cadmium(II) detection and capturing from wastewater. *Microchem. J.* **2021**, *164*, No. 105967.

(33) (a) Shahat, A.; Awual, M. R.; Khaleque, M. A.; Alam, M. Z.; Naushad, M.; Chowdhury, A.M.S. Large-pore diameter nano-adsorbent and its application for rapid lead(II) detection and removal from aqueous media. *Chem. Eng. J.* **2015**, *273*, 286−295. (b) Shahat, A.; Awual, M. R.; Naushad, M. Functional ligand anchored nanomaterial based facial adsorbent for cobalt(II) detection and removal from water samples. *Chem. Eng. J.* **2015**, *271*, 155−163. (c) Sharavanan, V. J.; Sivaramakrishnan, M.; Sivarajasekar, N.; Senthilrani, N.; Kothandan, R.; Dhakal, N.; Sivamani, S.; Show, P. L.; Awual, M. R.; Naushad, M. Pollutants inducing epigenetic changes and diseases. *Environ. Chem. Lett.* **2020**, *18*, 325−343. (d) Shahat, A.; Hassan, H.M.A.; Azzazy, H.M.E.; Hosni, M.; Awual, M. R. Novel nano-conjugate materials for effective arsenic(V) and phosphate capturing in aqueous media. *Chem. Eng. J.* **2018**, *331*, 54−63. (e) Salman, M. S.; Hasan, M. N.; Kubra, K. T.; Hasan, M. M. Optical detection and recovery of Yb(III) from waste sample using novel sensor ensemble nanomaterials. *Microchem. J.* **2021**, *162*, No. 105868.

(34) Langmuir, I. The constitution and fundamental properties of solids and liquids. Part I. Solids. *J. Am. Chem. Soc.* **1916**, *38*, 2221−2295.

(35) Freundlich, H.M.F. Over the adsorption in solution. *J. Phys. Chem. A* **1906**, *57*, 385−471.

(36) Dubinin, M. The equation of the characteristic curve of activated charcoal. *Proc. Acad. Sci. USSR Phys. Chem. Sect.* **1947**, *55*, 327−329.

(37) Tempkin, V. P. M. I. Kinetics of ammonia synthesis on promoted iron catalyst. *Acta Phys. Chim. USSR* **1940**, *12*, 327−356.

(38) (a) Shahat, A.; Hassan, H.M.A.; El-Shahat, M. F.; El Shahawy, O.; Awual, M. R. Visual nickel(II) ions treatment in petroleum samples using a mesoporous composite adsorbent. *Chem. Eng. J.* **2018**, *334*, 957−967. (b) Shahat, A.; Hassan, H.M.A.; Azzazy, H.M.E.; El-Sharkawy, E. A.; Abdou, H. M.; Awual, M. R. Novel hierarchical composite adsorbent for selective lead(II) ions capturing from wastewater samples. *Chem. Eng. J.* **2018**, *332*, 377−386. (c) Teo, S. H.; Islam, A.; Chan, E. S.; Thomas Choong, S.; Choong, S.Y.T.; Alharthi, N. H.; Taufiq-Yap, Y. H. Efficient biodiesel production from Jatropha curcus using $CaSO_4/Fe_2O_3$-SiO_2 core-shell magnetic nano-particles. *J. Clean. Prod.* **2019**, *208*, 816−826. (d) Rahman, M. M.; Awual, M. R.; Asiri, A. M. Preparation and evaluation of composite hybrid nanomaterials for rare-earth elements separation and recovery. *Sep. Purif. Technol.* **2020**, *253*, No. 117515. (e) Teo, S. H.; Islam, A.; Taufiq-Yap, Y. H.; Awual, M. R. Introducing the novel composite photocatalysts to boost the performance of hydrogen (H_2) production. *J. Clean. Prod.* **2021**, *313*, No. 127909.

(39) (a) Yeamin, M. B.; Islam, M. M.; Chowdhury, A. N.; Awual, M. Efficient encapsulation of toxic dyes from wastewater using several biodegradable natural polymers and their composites. *J. Clean. Prod.* **2021**, *291*, No. 125920. (b) Znad, H.; Abbas, K.; Hena, S.; Awual, M. R. Synthesis a novel multilamellar mesoporous TiO2/ZSM-5 for photo-catalytic degradation of methyl orange dye in aqueous media. *J. Environ. Chem. Eng.* **2018**, *6*, 218−227. (c) Kubra, K. T.; Salman, M. S.; Hasan, M. N.; Islam, A.; Hasan, M. M.; Awual, M. R. Utilizing an alternative composite material for effective copper(II) ion capturing from wastewater. *J. Mol. Liq.* **2021**, *336*, No. 116325. (d) Islam, A.; Teo, S. H.; Taufiq-Yap, Y. H.; Vo, D.V.N.; Awual, M. R. Towards the robust hydrogen (H_2) fuel production with niobium complexes-A review. *J. Clean. Prod.* **2021**, *318*, No. 128439. (e) Islam, A.; Teo, S. H.; Taufiq-Yap, Y. H.; Ng, C. H.; Vo, D.V.N.; Ibrahim, M. L.; Hasan, M. M.; Khan, M.A.R.; Nur, A.S.M. Step towards the sustainable toxic dyes and heavy metals removal and recycling from aqueous solution- A comprehensive review. *Resour. Conserv. Recy.* **2021**, *175*, No. 105849.

(40) (a) Miah, M. R.; Yang, M.; Hossain, M. M.; Khandaker, S.; Awual, M. R. Textile-based flexible and printable sensors for next generation uses and their contemporary challenges: A critical review. *Sensor. Actuat. A: Phy.* **2022**, *344*, No. 113696. (b) Kabir, M. M.; Akter, M. M.; Khandaker, S.; Gilroyed, B. H.; Didar-ul-Alam, M.; Alam, M. D.; Hakim, M. Highly effective agro-waste based functional green adsorbents for toxic chromium(VI) ion removal from wastewater. *J. Mol. Liq.* **2022**, *347*, No. 118327. (c) Teo, S. H.; Ng, C. H.; Islam, A.; Abdulkareem-Alsultan, G.; Joseph, C. G.; Janaun, J.; Taufiq-Yap, Y. H.; Taufiq-Yap, Y. H.; Khandaker, S.; Islam, G. J.; Znad, H. Sustainable toxic dyes removal with advanced materials for clean water production: A comprehensive review. *J. Clean. Prod.* **2022**, *332*, No. 130039. (d) Khandaker, S.; Das, S.; Hossain, M. T.; Islam, A.; Miah, M. R.; Awual, M. R. Sustainable approach for wastewater treatment using microbial fuel cells and green energy generation- A comprehensive review. *J. Mol. Liq.* **2021**, *344*, No. 117795. (e) Khandaker, S.; Hossain, M. T.; Saha, P. K.; Rayhan, U.; Islam, A.; Choudhury, T. R.; Awual, M. R. Functionalized layered double hydroxides composite bio-adsorbent for efficient copper(II) ion encapsulation from wastewater. *J. Environ. Manage.* **2021**, *300*, No. 113782.

(41) (a) Islam, A.; Swaraz, A. M.; Teo, S. H.; Taufiq-Yap, Y. H.; Vo, D.V.N.; Ibrahim, M. L.; Abdulkreem-Alsultan, G.; Rashid, U.; Awual, M. R. Advances in physiochemical and biotechnological approaches for sustainable metal recovery from e-waste: A critical review. *J. Clean. Prod.* **2021**, *323*, No. 129015. (b) Islam, A.; Teo, S. H.; Ng, C. H.; Taufiq-Yap, Y. H.; Choong, S.Y.T.; Awual, M. R. Progress in recent sustainable materials for greenhouse gas (NO_x and SO_x) emission mitigation. *Prog. Mater. Sci.* **2023**, *132*, No. 101033. (c) Hasan, M. N.; Salman, M. S.; Hasan, M. M.; Kubra, K. T.; Sheikh, M. C.; Rehan, A. I.; Rasee, A. I.; Waliullah, R. M.; Hossain, M. S.; Islam, A.; Khandaker, S.; Alsukaibi, A.K.D.; Alshammari, H. M.; et al. Assessing sustainable Lutetium(III) ions adsorption and recovery using novel composite hybrid nanomaterials. *J. Mol. Struct.* **2023**, *1276*, No. 134795. (d) Hossain, M. T.; Khandaker, S.; Bashar, M. M.; Islam, A.; Ahmed, M.; Akter, R.; Alsukaibi, A.K.D.; Hasan, M. M.; Alshammari, H. M.; Kuba, T.; Awual, M. R. Simultaneous toxic Cd(II) and Pb(II) encapsulation from contaminated water using Mg/Al-LDH composite materials. *J. Mol. Liq.* **2022**, *368*, No. 120810. (e) Miah, M. R.; Yang, M.; Khandaker, S.; Bashar, M. M.; Alsukaibi, A.K.D.; Hassan, H.M.A.; Znad, H.; Awual, M. R. Polypyrrole-based sensors for volatile organic compounds (VOCs) sensing and capturing: A comprehensive review. *Sensor. Actuat. A: Phys.* **2022**, *347*, No. 113933.

(42) Lagergren, S. K. About the theory of so-called adsorption of soluble substances. *Sven. Vetenskapsakad. Handingarl* **1898**, *24*, 1−39.

(43) Ho, Y.-S.; McKay, G. Pseudo-second order model for sorption processes. *J Process Biochem.* **1999**, *34*, 451−465.

(44) Vlad, M.; Segal, E. A kinetic analysis of Langmuir model for adsorption within the framework of Jovanovic theory; a generalization of the Jovanovic isotherm. *J. Surf. Sci.* **1979**, *79*, 608−616.

(45) (a) Zeldowitsch, J. The catalytic oxidation of carbon monoxide on manganese dioxide. *Acta Physicochim. URSS* **1934**, *1*, 364−449. (b) Al-Hazmi, G. H.; Refat, M. S.; Alshammari, K. F.; Kubra, K. T.; Shahat, A. Efficient toxic doxorubicin hydrochloride removal from aqueous solutions using facial alumina nanorods. *J. Mol. Struct.* **2023**, *1272*, No. 134187. (c) Rahman, M. M.; Wahid, A.; Asiri, A. M.; Awual, M. R.; Karim, M. R. One-step facile synthesis of SnO2@Nd2O3 nanocomposites for selective amidol detection in aqueous phase. *New J. Chem.* **2020**, *44*, 4952−4959. (d) Sheikh, T. A.; Rahman, M. M.; Asiri, A. M.; Marwani, H. M.; Awual, M. R. 4-Hexylresorcinol sensor development based on wet-chemically prepared Co3O4@Er2O3 nanorods: A practical approach. *J. Ind. Eng. Chem.* **2018**, *66*, 446−455. (e) Rahman, M. M.; Alamry, K. A.; Awual, M. R.; Mekky, A.E.M. Efficient Hg(II) ionic probe development based on one-step synthesized diethyl thieno[2,3-b]thiophene-2,5-dicarboxylate (DETTDC2) onto glassy carbon electrode. *Microchem. J.* **2020**, *152*, No. 104291.

(46) Al-Hazmi, G. A. A.; El-Bindary, M. A.; El-Desouky, M. G.; El-Bindary, A. A. Efcient adsorptive removal of industrial dye from aqueous solution by synthesized zeolitic imidazolate framework-8 loaded date seed activated carbon and statistical physics modeling. *Desalin. Water Treat.* **2022**, *258*, 85−103.

(47) (a) H Al-Hazmi, G.; Adam, A.M.A.; El-Desouky, M. G.; El-Bindary, A. A.; Alsuhaibani, A. M.; Refat, M. S. Efficient adsorption of Rhodamine B using a composite of Fe_3O_4@ zif-8: Synthesis, characterization, modeling analysis, statistical physics and mechanism

https://doi.org/10.1021/acsomega.3c00829
ACS Omega 2023, 8, 14144−14159

of interaction. *Bull. Chem. Soc. Ethiop.* **2022**, *37*, 211−229. (b) Awual, M. R.; Jyo, A.; Jyo, A.; El-Safty, S. A.; El-Safty, S. A.; Tamada, M.; Tamada, M.; Seko, N. A weak-base fibrous anion exchanger effective for rapid phosphate removal from water. *J. Hazard. Mater.* **2011**, *188*, 164−171. (c) Awual, M. R.; El-Safty, S. A.; El-Safty, S. A.; Jyo, A. Removal of trace arsenic(V) and phosphate from water by a highly selective ligand exchange adsorbent. *J. Environ. Sci.* **2011**, *23*, 1947−1954. (d) El-Safty, S. A.; Awual, M.; Shenashen, M. A.; Shahat, A. Simultaneous optical detection and extraction of cobalt(II) from lithium ion batteries using nanocollector monoliths. *Sens. Actuators, B* **2013**, *176*, 1015−1025. (e) El-Safty, S. A.; Shenashen, M. A.; Ismael, M.; Khairy, M.; Awual, M. R. Optical mesosensors for monitoring and removal of ultra-trace concentration of Zn(II) and Cu(II) ions from water. *Analyst* **2012**, *137*, 5278−5290.

(48) Al-Hazmi, G. H.; El-Desouky, M. G.; El-Bindary, A. A. Synthesis, characterization and microstructural evaluation of MSNP nanoparticles by William-Hall and size-strain plot methods. *Bull. Chem. Soc. Ethiop.* **2022**, *36*, 815−829.

(49) Altalhi, T. A.; Ibrahim, M. M.; Mersal, G. A.; Mahmoud, M.; Kumeria, T.; El-Desouky, M. G.; El-Bindary, A. A.; El-Bindary, M. A. Adsorption of doxorubicin hydrochloride onto thermally treated green adsorbent: Equilibrium, kinetic and thermodynamic studies. *J. Mol. Struct.* **2022**, *1263*, No. 133160.

(50) (a) Al-Hazmi, G. A. A.; El-Zahhar, A. A.; El-Desouky, M. G.; El-Bindary, M. A.; El-Bindary, A. A. Adsorption of industrial dye onto a zirconium metal-organic framework: synthesis, characterization, kinetics, thermodynamics, and DFT calculations. *J. Coord. Chem.* **2022**, *75*, 1203−1229. (b) Arshad, M. N.; Sheikh, T. A.; Rahman, M. M.; Asiri, A. M.; Marwani, H. M.; Awual, M. R. Fabrication of cadmium ionic sensor based on (E)-4-Methyl-N′-(1-(pyridin-2-yl) ethylidene) benzenesulfonohydrazide (MPEBSH) by electrochemical approach. *J. Organomet. Chem.* **2017**, *827*, 49−55. (c) Awual, M. R.; Jyo, A. Assessing of phosphorus removal by polymeric anion exchangers. *Desalination* **2011**, *281*, 111−117. (d) Awual, M. R.; Jyo, A. Rapid column-mode removal of arsenate from water by crosslinked poly(allylamine) resin. *Water Res.* **2009**, *43*, 1229−1236. (e) Awual, M. R.; Urata, S.; Jyo, A.; Tamada, M.; Katakai, A. Arsenate removal from water by a weak-base anion exchange fibrous adsorbent. *Water Res.* **2008**, *42*, 689−696.

(51) Al-Wasidi, A. S.; AlZahrani, I.IS.; Thawibaraka, H. I.; Naglah, A. M.; El-Desouky, M. G.; El-Bindary, M. A. Adsorption studies of Carbon dioxide and Anionic dye on Green Adsorbent. *J. Mol. Struct.* **2022**, *1250*, No. 131736.

(52) Hassan, N.; Shahat, A.; El-Didamony, A.; El-Desouky, M. G.; El-Bindary, A. A. Equilibrium, Kinetic and Thermodynamic studies of adsorption of cationic dyes from aqueous solution using ZIF-8. *Moroccan J. Chem.* **2020**, *8*, 2627−2637.

(53) Hassan, N.; SHahat, A.; El-Didamony, A.; El-Desouky, M. G.; El-Bindary, A. A. Synthesis and characterization of MSNP nanoparticles via zeolitic imidazolate framework-8 and its application for removal of dyes. *J. Mol. Struct.* **2020**, *1210*, No. 128029.

(54) (a) Dihan, M. R.; Abu Nayeem, S.; Nayeem, S. M. A.; Roy, H.; Islam, M. S.; Islam, A.; Alsukaibi, A.K.D. Healthcare waste in Bangladesh: Current status, the impact of Covid-19 and sustainable management with life cycle and circular economy framework. *Sci. Total Environ.* **2023**, *871*, No. 162083. (b) Rasel, H. M.; Al Mamun, M. A.; Hasnat, A.; Alam, S.; Hossain, I.; Mondal, R. K.; Good, R. Z.; Alsukaibi, A.K.D.; Awual, M. R. Sustainable futures in agricultural heritage: Geospatial exploration and predicting groundwater-level variations in *Barind* Tract of Bangladesh. *Sci. Total Environ.* **2023**, *865*, No. 161297. (c) Khandaker, S.; Bashar, M. M.; Islam, A.; Hossain, M. T.; Teo, S. H.; Awual, M. R. Sustainable energy generation from textile biowaste and its challenges: A comprehensive review. *Renewable Sustainable Energy Rev.* **2022**, *157*, No. 112051. (d) Hasan, M. M.; Kubra, K. T.; Hasan, M. N.; Salman, M. S.; Sheikh, M. C.; Rehan, A. I.; Rasee, A. I.; Waliullah, R. M.; Islam, M. S.; Khandaker, S.; Islam, A.; Hossain, M. S.; Alsukaibi, A. K. D.; Alshammari, H. M.; et al. Sustainable ligand-modified based composite material for the selective and effective cadmium(II) capturing from wastewater. *J. Mol. Liq.* **2023**, *371*, No. 121125. (e) Salman, M. S.; Hasan, M. N.; Hasan, M. M.; Kubra, K. T.; Sheikh, M. C.; Rehan, A. I.; Waliullah, R. M.; Rasee, A. I.; Hossain, M. S.; Alsukaibi, A.K.D.; Alshammari, H. M.; et al. Improving copper(II) ion detection and adsorption from wastewater by the ligand-functionalized composite adsorbent. *J. Mol. Struct.* **2023**, *1282*, No. 135259.

(55) (a) Rajendran, S.; Hoang, T.K.A.; Trudeau, M. L.; Jalil, A. A.; Naushad, M.; Awual, M. R. Generation of novel n-p-n (CeO_2-PPy-ZnO) heterojunction for photocatalytic degradation of micro-organic pollutants. *Environ. Pollut.* **2022**, *292*, No. 118375. (b) Islam, A.; Roy, S.; Teo, S. H.; Khandaker, S.; Taufiq-Yap, Y. H.; Aziz, A. A.; Monir, M. U.; Rashid, U.; Vo, D.V.N.; Ibrahim, M. L.; Znad, H.; Awual, M. R. Functional novel ligand based palladium(II) separation and recovery from e-waste using solvent-ligand approach. *Colloid. Surface. A: Physicochem. Eng. Aspect.* **2022**, *632*, No. 127767. (c) Awual, M. R.; Shenashen, M. A.; Jyo, A.; Shiwaku, H.; Yaita, T. Preparing of novel fibrous ligand exchange adsorbent for rapid column−mode trace phosphate removal from water. *J. Ind. Eng. Chem.* **2014**, *20*, 2840−2847. (d) Awual, M. R.; Khaleque, M. A.; Ferdows, M.; Chowdhury, A.M.S.; Yaita, T. Rapid recognition and recovery of gold(III) with functional ligand immobilized novel mesoporous adsorbent. *Microchem. J.* **2013**, *110*, 591−598. (e) El-Sayed, W. N.; Elwakeel, K. Z.; Shahat, A.; Awual, M. R. Investigation of novel nanomaterial for the removal of toxic substances from contaminated water. *RSC Adv.* **2019**, *9*, 14167−14175.

(56) (a) Al-tabatabaie, K. F.; Hossain, M. B.; Islam, M. K.; Awual, M. R.; Islam, A.R.M.T.; TowfiqulIslam, A. R. M.; Hossain, M. A.; Esraz-Ul-Zannat, M.; Islam, A. Taking strides towards decarbonization: The viewpoint of Bangladesh. *Energy Strategy Rev.* **2022**, *44*, No. 100948. (b) Shahat, A.; Mohamed, M. H.; Awual, M. R.; Mohamed, S. K. Novel and potential chemical sensors for Au(III) ion detection and recovery in electric waste samples. *Microchem. J.* **2020**, *158*, No. 105312. (c) Shahat, A.; El-Shahat, M. F.; El Shahawy, O. A ligand-anchored optical composite material for efficient vanadium(II) adsorption and detection in wastewater. *New J. Chem.* **2019**, *43*, 10324−10335. (d) Awual, M. R.; Hossain, M. A.; Shenashen, M. A.; Yaita, T.; Suzuki, S.; Jyo, A. Evaluating of arsenic(V) removal from water by weak-base anion exchange adsorbents. *Environ. Sci. Pollut. Res.* **2013**, *20*, 421−430. (e) Awual, M. R.; Shenashen, M. A.; Yaita, T.; Shiwaku, H.; Jyo, A. Efficient arsenic(V) removal from water by ligand exchange fibrous adsorbent. *Water Res.* **2012**, *46*, 5541−5550.

(57) (a) Znad, H.; Al-Mohammedawi, H.; Awual, M. R. Integrated pre-treatment stage of biosorbent-sonication for mixed brewery and restaurant effluents to enhance the photo-fermentative hydrogen production. *Biomass Bioenerg.* **2021**, *144*, No. 105899. (b) Ismael, M. Efficient gold(III) detection, separation and recovery from urban mining waste using a facial conjugate adsorbent. *Sens. Actuators, B* **2014**, *196*, 457−466. (c) Awual, M. R.; Yaita, T.; Okamoto, Y. A novel ligand based dual conjugate adsorbent for cobalt(II) and copper(II) ions capturing from water. *Sens. Actuators, B* **2014**, *203*, 71−80. (d) Ismael, M.; Yaita, T. Efficient detection and extraction of cobalt(II) from lithium ion batteries and wastewater by novel composite adsorbent. *Sens. Actuators, B* **2014**, *191*, 9−18. (e) Mohamed, S. K.; Hassan, H. M. A.; Shahat, A.; Awual, M. R.; Kamel, R. M. A ligand-based conjugate solid sensor for colorimetric ultra-trace gold(III) detection in urban mining waste. *Colloid. Surface A* **2019**, *581*, No. 123842.

(58) Chudoba, D.; Łudzik, K.; Jażdżewska, M.; Wołoszczuk, S. Kinetic and equilibrium studies of doxorubicin adsorption onto carbon nanotubes. *Int. J. Mol. Sci.* **2020**, *21*, 8230.

(59) El-Desouky, M. G.; El-Bindary, M. A.; El-Bindary, A. A. Effective adsorptive removal of anionic dyes from aqueous solution. *Vietnam J. Chem.* **2021**, *59*, 341−361.

(60) El-Desouky, M. G.; Hassan, N.; Shahat, A.; El-Didamony, A.; El-Bindary, A. A. Synthesis and characterization of porous magnetite nanosphere iron oxide as a novel adsorbent of anionic dyes removal from aqueous solution. *Biointerface Res. Appl. Chem.* **2021**, *11*, 13377−13401.

(61) Altalhi, T. A.; Ibrahim, M. M.; Mersal, G. A.; Mahmoud, M.; Kumeria, T.; El-Desouky, M. G.; El-Bindary, A. A.; El-Bindary, M. A. Adsorption of doxorubicin hydrochloride onto thermally treated green

https://doi.org/10.1021/acsomega.3c00829
ACS Omega 2023, 8, 14144−14159

adsorbent: Equilibrium, kinetic and thermodynamic studies. *J. Mol. Struct.* **2022**, *1263*, No. 133160.
(62) AlHazmi, G. A.; AbouMelha, K. S.; El-Desouky, M. G.; El-Bindary, A. A. Effective Adsorption of Doxorubicin Hydrochloride on Zirconium Metal-Organic Framework: Equilibrium, Kinetic and Thermodynamic Studies. *J. Mol. Struct.* **2022**, *1258*, No. 132679.
(63) Wu, S.; Zhao, X.; Li, Y.; Du, Q.; Sun, J.; Wang, Y.; Wang, X.; Xia, Y.; Wang, Z.; Xia, L. Adsorption properties of doxorubicin hydrochloride onto graphene oxide: equilibrium, kinetic and thermodynamic studies. *Materials* **2013**, *6*, 2026−2042.
(64) Al-Hazmi, G. A. A.; El-Zahhar, A. A.; El-Desouky, M. G.; El-Bindary, M. A.; El-Bindary, A. A. Efficiency of Fe_3O_4@ ZIF-8 for the removal of Doxorubicin from aqueous solutions: Equilibrium, kinetics and thermodynamic studies. *J. Environ. Technol.* **2022**, 1−48.

https://doi.org/10.1021/acsomega.3c00829
ACS Omega 2023, 8, 14144−14159